BIOGEOCHEMISTRY OF A GLACIATED FJORD ECOSYSTEM: GLACIER BAY NATIONAL PARK, ALASKA

By

Stacey Reisdorph

RECOMMENDED:

Dr. Ana Aguilar-Islas

Dr. Seth Danielson

Dr. Eran Hood

Dr. Jeremy Mathis
Advisory Committee Co-Chair

Dr. Thomas Weingartner
Advisory Committee Co-Chair

Dr. Katrin Iken
Program Head, Marine Science and Limnology

APPROVED:

Dr. Joan Braddock
Interim Dean, School of Fisheries and Ocean Sciences

Dr. John Eichelberger
Dean of the Graduate School

13 March 2015
Date

BIOGEOCHEMISTRY OF A GLACIATED FJORD ECOSYSTEM: GLACIER BAY NATIONAL PARK, ALASKA

A

THESIS

Presented to the Faculty

of the University of Alaska Fairbanks

in Partial Fulfillment of the Requirements

for the Degree of

MASTER OF SCIENCE

By

Stacey Reisdorph, B.A., B.S.

Fairbanks, Alaska

May 2015

Abstract

The burning of fossil fuels, coupled with land use and deforestation practices, has resulted in CO_2 being emitted into the atmosphere. As much as one third of the anthropogenic, or man-made, CO_2 that ends up in the atmosphere is absorbed by the oceans and has led to increases in marine dissolved inorganic carbon (DIC) concentrations and a decrease in ocean pH, a process referred to as ocean acidification (OA). Increased concentrations of DIC can reduce saturation states (Ω) with respect to biologically important calcium carbonate minerals, such as aragonite. However, CO_2 may not be the only factor in seasonal changes to calcium carbonate saturation states. With this project I was interested in understanding how glacial runoff impacts the seasonal changes to the marine biogeochemistry in a glaciated fjord. In addition to CO_2, glacial meltwater is low in alkalinity (TA) and may impact the seasonal biogeochemistry of the marine system, as well as how it influences the duration, extent, and severity of OA events in an Alaskan glacial fjord, Glacier Bay National Park (GLBA). Through this study, I found that glacial runoff heavily impacts aragonite saturation states, with the main drivers of Ω (DIC and TA) varying seasonally. In GLBA low Ω values were well correlated with the timing of maximum glacial discharge events and most prominent within the two regions where glacial discharge was highest.

The influence of glaciers is not limited to just TA as runoff is also low in macronutrients due to a lack of leaching from the soil and rocky streambeds. This has the potential to greatly impact the efficiency and structure of the marine food web within GLBA, the lowest level of which can be estimated using net community production (NCP). Changes within the lowest level of the food web, as a result of seasonal OA events, may lead to bottom-up effects throughout the food web, though this project focused only on production and respiration signals within the lowest level. We estimated regional NCP values for each sampling season and found the highest NCP rates (~54 to ~81 mmoles C m^{-2} d^{-1}) between the summer and fall of 2011, with the most marine influenced lower part of the bay experiencing the greatest production.

As the climate continues to warm, further glacial volume loss will likely lead to additional modifications in the carbon biogeochemistry of GLBA. Understanding the dynamics that drive seasonal changes in Ω, NCP, and the associated air-sea CO_2 fluxes within glacially influenced Alaskan fjords can provide insights into how deglaciation may affect carbon budgets and production in similar fjords worldwide.

Table of Contents

List of Figures

Page

List of Tables

Page

Acknowledgements

Thanks to the National Park Service for supporting this work through grant number G7224 to the University of Alaska Fairbanks. I want to thank my committee members, Dr. Jeremy Mathis (UAF-SFOS/PMEL), Dr. Ana Aguilar-Islas (UAF-SFOS), Dr. Tom Weingartner (UAF-SFOS), Dr. Seth Danielson (UAF-SFOS), and Dr. Eran Hood (UAS) for all of the their time and guidance. I also want thank Lewis Sharman (NPS-GLBA), Natalie Monacci (UAF-OARC), Jessica Cross (UAF-SFOS/PMEL), Chase Stoudt (UAF-SFOS) and NPS staff members in Gustavus and Juneau, AK for their help in sample collection, logistics and editing. I want to thank the staff and visitors of Glacier Bay National Park and Preserve, as well as the community of Gustavus for their support and interest in this project. For this project, Dr. Jeremy Mathis prepared the project proposal for funding and designed the sampling protocols. I completed the fieldwork, in-field and laboratory sampling analyses, and wrote the manuscripts; revisions and editing were done with assistance by Dr. Mathis.

Chapter 1: General Introduction

Alaska's coasts contain more than 200 major fjords, though few have been studied in detail with respect to their biogeochemistry (Etherington et al., 2007). Glacier Bay National Park and Preserve (GLBA) lies along the eastern coast of the Gulf of Alaska (GOA) in Southeast Alaska and is an example of a pristine glacial fjord ecosystem. GLBA was once occupied by one large icefield, aptly named the Glacier Bay Icefield, that has experienced rapid deglaciation since the end of the Little Ice Age (LIA), circa AD1770 (Larsen et al., 2005; Johnson et al., 2013). As a result of this deglaciation, GLBA is now surrounded by a multitude of tidewater and alpine glaciers.

Since the end of the LIA and the start of the Industrial Revolution in the late 18th century, mankind has emitted a large volume of carbon dioxide (CO_2) into the atmosphere, primarily from the burning of fossil fuel, as well as cement production and changing land-use practices, including deforestation and the use of crop pesticides (Sabine et al., 2004). Rising levels of greenhouse gases, such as CO_2 have the potential to increase the global surface temperatures by as much as 1 to 6° C by 2100 (Ryu and Jacobson, 2012).

The CO_2 emitted into the atmosphere gets partitioned between the atmosphere, terrestrial and marine ecosystems. Approximately 46% of anthropogenic CO_2 remains in the atmosphere, while ~28% is taken up by the terrestrial biosphere, and the remaining ~26% is taken up by the ocean (Sabine et al., 2004; Cai et al., 2010). This increase in oceanic CO_2 has led to an increase in dissolved inorganic carbon (DIC) concentrations, a reduction in global ocean pH of ~0.1 units (Feely et al., 2004), referred to as ocean acidification (OA). In addition, it led to a reduction in saturation states (Ω) with respect to biologically important calcium carbonate minerals, such as calcite and aragonite (Mucci, 1983). Saturation states can also be influenced by changes in total alkalinity (TA) concentrations, especially within the coastal ocean and estuarine ecosystems where low-TA freshwater and glacial inputs are higher (Feely et al., 2010; Mathis et al., 2011; Evans and Mathis, 2013). The marine ecosystem in GLBA, as well as in numerous similar fjord systems along the GOA, are highly influenced by freshwater runoff from the many surrounding alpine and tidewater glaciers. The significant volume of low-TA, low-nutrient freshwater runoff into GLBA, highest along the northern regions of the bay, impacts DIC and TA concentrations as well as nutrient loading. These processes subsequently affect biological production within the bay.

Global temperature rise along with climate patterns such as the Pacific Decadal Oscillation (PDO), El Niño-Southern Oscillation (ENSO), and the Arctic Oscillation (AO), act to impact marine systems through changes in physical forcings, including regional winds, freshwater flux, and seawater temperature. In turn, these physical forcings influence nutrient supply, stratification, and the timing and extent of phytoplankton blooms (Stabeno et al., 2004). Since ~1977, the regions around Alaska have been experiencing a positive PDO phase, with minor deviations into a negative phase in the early 1980s and late 2000s. The positive PDO phase is characterized by higher temperatures and higher precipitation in maritime regions of Alaska, such as GLBA (Arendt et al., 2009). The AO has experienced more frequent fluctuations than the PDO, with a large negative-to-positive shift in 1989. A positive AO causes a strong polar vortex that prohibits cold, polar air from reaching lower latitudes (Arendt et al., 2009). The coupling of these systems with anthropogenic CO_2 can exacerbate warming, increasing atmospheric temperatures and leading to greater glacial runoff and volume loss.

Watersheds along the GOA are experiencing climate warming and glacier loss (Neal et al., 2010). Using altimetry data, Arendt et al. (2009) noted that the majority of Alaskan and northwestern Canadian glaciers have been losing mass over the past 50 years and that the average rate of loss has increased since the mid–1990s. They also noted that between 1950 and 2002, air temperatures in Alaska and northwestern Canada have increased, with the largest increase observed during the winter (1.0° ± 0.4°C increase in summer vs. 2.0° ± 0.8°C during winter within their study area). Arendt et al. (2009) suggest that the increase in summer temperatures is driving the rates of glacier mass loss in Alaska and northwestern Canada. In maritime glaciers at elevations near sea level, such as those in GLBA, may melt not only in the summer but also during the winter (Arendt et al., 2009). In terms of tidewater glaciers, a crucial factor in GLBA's biogeochemistry, initial tidewater glacier retreat may begin as a result of climatic change, though once initiated, can continue independently of climate (Meier and Post, 1987).

As a result of the numerous glaciers surrounding GLBA, the bay is highly influenced by glacier melt and freshwater runoff, particularly in its northern regions where glacial input is greatest. GLBA experiences a moderate maritime climate averaging 1.9 m of precipitation annually in Bartlett Cove, near the entrance of the bay (Hooge and Hooge, 2002). Multiple glacier mass balance studies have found that glaciers in wetter, maritime climates, like that of

GLBA, tend to have an increased sensitivity to temperature and precipitation changes than those within subpolar or continental climates (Radić and Hock, 2014). GLBA currently has eight tidewater glaciers and numerous alpine glaciers covering an area of ~ 6428 km^2 as of August 2010, though the majority of glaciers in GLBA are experiencing mass loss (Johnson et al., 2013). This glacial volume loss adds low-TA, nutrient-poor freshwater to the bay, which influences physical, chemical and biological aspects of the marine system.

GLBA communicates with marine waters of the GOA across a shallow sill (~25 m) (Etherington et al., 2007) via several small channels, including Cross Sounds and Icy Strait (Hill et al., 2009). Despite GLBA's limited deep-water exchange with the open ocean and input from glacial runoff, it experiences elevated chlorophyll-*a* (chl. *a*) concentrations throughout most of the year, particularly from spring through fall (Etherington et. al., 2007). Primary production throughout the bay supports a diverse food web, including endangered species such as humpback whales and Stellar sea lions. As climate change continues, further glacial retreat will likely lead to additional modifications in the carbon biogeochemistry of GLBA with unknown consequences for marine food web. These changes in the marine carbon biogeochemistry are likely to have an impact on the net community production (NCP) within the bay, with cascading effects through all levels of the food web. For example, glacial retreat along the GOA has been linked to decreasing populations of capelin, an important forage fish that can be found in GLBA and prefers the colder waters near tidewater glacier outflows and attracts many marine predators (Arimitsu et al., 2008). In order to estimate how deglaciation and glacial runoff influence the biogeochemistry of the GLBA, I analyzed seasonal rates of NCP and identified how glacial runoff is currently influencing the marine chemistry and degree of seasonal OA in GLBA. Understanding the dynamics that drive NCP, air-sea CO_2 fluxes and carbon biogeochemistry within glacially influenced Alaskan fjords can provide insights on how deglaciation may affect carbon budgets and OA in fjords worldwide.

1.1 References

Arendt, A., Walsh, J., Harrison, W., 2009. Changes of glaciers and climate in northwestern North America during the late twentieth century. J. Clim., 22, 4117–4134. doi:10.1175/2009JCLI2784.1

Arimitsu, M.L., Piatt, J.F., Litzow, M.A., Abookire, A.A., Romano, M.D., Robards, M.D., 2008. Distribution and spawning dynamics of capelin (*Mallotus villosus*) in Glacier Bay, Alaska: a cold water refugium. Fish. Oceanogr., 17, 137–146. doi:10.1111/j.1365-2419.2008.00470

Cai, W.J., Chen, L., Chen, B., Gao, Z., Lee, S.H., Chen, J., Pierrot, D., Sullivan, K., Wang, Y., Hu, X., Huang, W.-J., Zhang, Y., Xu, S., Murata, A., Grebmeier, J.M., Jones, E.P., Zhang, H., 2010. Decrease in the CO_2 uptake capacity in an ice-free Arctic Ocean basin. Science, 329, 556–559. doi:10.1126/science.1189338

Etherington, L., Hooge, P.N., Hooge, E.R., Hill, D.F., 2007. Oceanography of Glacier Bay, Alaska: implications for biological patterns in a glacial fjord estuary. Estuar. & Coasts, 30, 927–944.

Evans, W., Mathis, J.T., 2013. The Gulf of Alaska coastal ocean as an atmospheric CO_2 sink. Cont. Shelf Res., 65, 52–63. doi:10.1016/j.csr.2013.06.013

Feely, R.A, Sabine, C.L., Lee, K., Berelson, W., Kleypas, J., Fabry, V.J., Millero, F.J., 2004. Impact of anthropogenic CO_2 on the $CaCO_3$ system in the oceans. Science, 305, 362–366. doi:10.1126/science.1097329

Feely, R.A., Alin, S.R., Newton, J., Sabine, C.L., Warner, M., Devol, A., Krembs, C., Maloy, C., 2010. The combined effects of ocean acidification, mixing, and respiration on pH and carbonate saturation in an urbanized estuary. Estuar. Coast. Shelf Sci., 88, 442–449. doi:10.1016/j.ecss.2010.05.004

Hill, S.J., Ciavola, L., Etherington, M.J., Klaar, D.F., 2009. Estimation of freshwater runoff into Glacier Bay, Alaska and incorporation into a tidal circulation model. Estuar. Coast. Shelf Sci., 82, 95–107.

Hooge, E.R., Hooge, P.N., 2002. Fjord oceanographic processes in Glacier Bay, Alaska. Glacier Bay Rep., Gustavus, AK, 1-144.

Johnson, A.J., Larsen, C.F., Murphy, N., Arendt, A.A., Zirnheld, S.L., 2013. Mass balance in the Glacier Bay area of Alaska, USA, and British Columbia, Canada, 1995–2011, using airborne laser altimetry. Jour. Glac., 59, 632–648. doi:10.3189/2013JoG12J101

Larsen, C.F., Motyka, R.J., Freymueller, J.T., Echelmeyer, K. A., Ivins, E.R., 2005. Rapid viscoelastic uplift in southeast Alaska caused by post-Little Ice Age glacial retreat. Earth Planet. Sci. Lett., 237, 548–560. doi:10.1016/j.epsl.2005.06.032

Mathis, J.T., Cross, J.N., Bates, N.R., 2011. The role of ocean acidification in systemic carbonate mineral suppression in the Bering Sea. Geophys. Res. Lett., 19, 1-6. doi:10.1029/2011GL048884.

Meier, M.F., Post, A., 1987. Fast tidewater glaciers. J. Geophys. Res., 92, 9051–9058. doi:10.1029/JB092iB09p09051

Mucci, A., 1983. The solubility of calcite and aragonite in seawater at various salinities, temperatures, and one atmosphere total pressure. Amer. Jour. of Sci., 283, 780-799.

Neal, E.G., Hood, E., Smikrud, K., 2010. Contribution of glacier runoff to freshwater discharge into the Gulf of Alaska. Geophys. Res. Lett., 37, 1-5. doi:10.1029/2010GL042385

Radić, V., Hock, R., 2014. Glaciers in the earth's hydrological cycle: assessments of glacier mass and runoff changes on global and regional scales. Surv. Geophys., 35, 813–837. doi:10.1007/s10712-013-9262-y

Ryu, J.S., Jacobson, A.D., 2012. CO_2 evasion from the Greenland Ice Sheet: A new carbon-climate feedback. Chem. Geol., 320-321, 80–95. doi:10.1016/j.chemgeo.2012.05.024

Sabine, C.L., Feely, R.A., Gruber, N., Key, R.M., Lee, K., Bullister, J.L., Wanninkhof, R., Wong, C.S., Wallace, D.W.R., Tilbrook, B., Millero, F.J., Peng, T. H., Kozyr, A., Ono, T., Rios, A.F., 2004. The oceanic sink for anthropogenic CO_2. Science, 305, 367-371. doi:10.1126/science.1097403

Stabeno, P., Bond, N., Hermann, A., Kachel, N., Mordy, C., Overland, J., 2004. Meteorology and oceanography of the Northern Gulf of Alaska. Cont. Shelf Res., 24, 859–897. doi:10.1016/j.csr.2004.02.00

CHAPTER 2:

The Dynamic Controls on Carbonate Mineral Saturation States and Ocean Acidification in a Glacially Dominated Estuary[1]

2.0 Abstract

Recently, a number of studies have shown that the intrusion of anthropogenic carbon dioxide (CO_2) into the ocean has created an acidification effect leading to the reduction in carbonate mineral saturation states (Ω). However, the uptake of atmospheric CO_2 is not the only climate-induced phenomenon that leads to a reduction of Ω in marine environments. Over the past ~250 years, Glacier Bay, AK (GLBA) has experienced rapid deglaciation leading to an increase in the amount of freshwater entering the marine ecosystem. This excess freshwater discharge is low in total alkalinity and reduces the buffering capacity of surface waters and enhances the vulnerability of the estuary to further reductions in pH. The corresponding reduction in Ω may cause these waters to become corrosive to shell-building organisms. To better understand these processes, we collected monthly samples within GLBA that show the variability in Ω throughout the water column. Low Ω values were well correlated with the timing of maximum glacial discharge events and most prominent within the two regions where tidewater glacial discharge was highest. The saturation state with respect to aragonite reached a minimum of 0.40 at the surface during the summer of 2011 before rebounding to a maximum value of 3.26 in the spring of 2012. Aragonite was undersaturated at the surface throughout the entire bay during fall months (Sept. and Oct.). Here, we present results from a year-long study designed to constrain the effects of glacial freshwater discharge on the marine carbonate system and discern the primary controls on Ω in this pristine estuarine environment.

2.1 Introduction

Since the onset of the Industrial Revolution, the oceans have taken up roughly one third of all anthropogenic carbon dioxide (CO_2) emitted into the atmosphere (Sabine et al., 2004; Cai et al., 2010). This uptake of anthropogenic CO_2 has already caused an increase in oceanic dissolved inorganic carbon (DIC) concentrations leading to a decrease in global surface ocean pH of ~0.1 units (Feely et al., 2004). The reduction in marine pH is referred to as ocean acidification (OA) and it has caused a decline in the saturation state (Ω) of biologically important

calcium carbonate minerals, such as calcite and the less stable aragonite (Mucci, 1983). However, the uptake of CO_2 by the oceans is not the only process that can reduce Ω in seawater. Saturation states can also be affected by changes in total alkalinity (TA) concentrations, particularly in the coastal ocean and estuaries, where DIC/TA-salinity relationships are largely non-conservative (i.e., Feely et al., 2010; Mathis et al., 2011a; Evans et al., 2014). Although these are the two major influences on changes in Ω, there are also smaller perturbations to the carbonate system (i.e., calcification, nutrient uptake and respiration) that can have minor impacts on Ω (e.g., Cross et al, 2013). Changes in DIC can be attributed to primary production, respiration, calcification and dissolution of calcium carbonate ($CaCO_3$), while changes in TA can be caused by dissolution of $CaCO_3$, denitrification, and changes in the volume of freshwater runoff entering the marine environment (Cai et al., 2004; Cai et al., 2010). These processes can be particularly intense in high latitude estuarine and coastal zones where there are large seasonal gradients in freshwater fluxes, nutrient delivery and light intensity (Mathis et al., 2011a; Cross et al., 2013).

Glacier Bay (Figure 2.1) is a pristine glacial fjord that is representative of much of the coastal domain of the eastern Gulf of Alaska (GOA). It is largely influenced by freshwater runoff from its many glaciers, including seven tidewater glaciers. These glaciers were once part of the large Glacier Bay Icefield that has experienced a very rapid retreat since the Little Ice Age, which ended in the late 18th century (Barclay et al., 2001; Arendt et al., 2002; Larsen et al., 2005). As the icefield retreated, it left behind many smaller glaciers, seven of which are still active tidewater glaciers and two of which are currently advancing or stable (Johnson et al., 2013). Over the past ~250 years, GLBA has experienced some of the most rapid deglaciations on record (Goodwin, 1988; Pfeffer et al., 2000), increasing the amount of freshwater runoff into the marine ecosystem, thus affecting the chemistry, biology and flow dynamics in the bay (Hill et al., 2009). Studies of tidewater glacial runoff in other locations have shown that these waters are low in TA relative to marine waters (Mathis et al., 2011a; Evans et al, 2014). Enhanced runoff due to anthropogenically induced warming or natural changes in the hydrological cycle could drive a non-CO_2 reduction effect for Ω in the western GOA. Here, we use a new and unprecedented dataset of seasonal observations across GLBA to elucidate the controls on carbonate mineral saturations states in the region.

2.2 Background

GLBA has a moderate maritime climate averaging 1.9 m of precipitation annually in Bartlett Cove (Figure 2.1), at the entrance of the bay (Hooge and Hooge, 2002). Etherington et al. (2007) found precipitation rates to be highest in September and October (0.94 and 1.01 cm d^{-1}, respectively), with the lowest precipitation occurring in May (0.31 cm d^{-1}) and June (0.28 cm d^{-1}). Summer climate is characterized by weak high-pressure systems that form over the area and bring warmer temperatures and limited cloud cover. The steep topography around GLBA creates many hundreds of small ephemeral streams that contribute to the freshwater runoff of the bay (Hill et al., 2009).

GLBA is connected to the marine waters of the GOA though several small channels (Hill et al., 2009) (Figure 2.1). The deepest area of the bay is along a roughly north–south trough that runs from central bay up the west arm, where bottom depths can reach ~450 m. Ventilation of these waters from the GOA takes place across a shallow (~25 m) sill at the entrance of bay. The main channel bifurcates into two smaller arms, both of which terminate at large glaciers at their northern extents, with the west arm terminating at a tidewater glacier face. There is a shallow sill (~ 60 m) at the entrance to east arm that may limit some exchange between the arm and the main channel (Hooge and Hooge, 2002). GLBA is typically divided into four sub-regions (Figure 2.1): the lower bay (LB), which includes the mouth of the bay as well Icy Strait and Cross Sound, the central bay (CB), an east arm (EA), and a west arm (WA).

GLBA's circulation is tidally influenced with a mixed semi-diurnal cycle at a range averaging 3.7 m in Bartlett Cove to 4.3 m halfway into each arm (Hooge and Hooge, 2002). Several acoustic Doppler current profiler (ADCP) transects along the length of the bay (Cokelet et al., 2007) found the greatest current speeds at the choke-point over the entrance sill (180 cm s^{-1}) with these flows slowing on the bay-side of the sill to a few cm s^{-1}. They suggested that strong currents across this shallow entrance sill mix nutrient-rich waters from depth into the surface layer and supply nutrients to the bay.

During winter months (January–March) the water column is well mixed. In spring, increased precipitation and glacial runoff deepen the pycnocline until it reaches the outer sill depth and limits the exchange of the denser bottom waters with marine waters outside the bay. Matthews (1981) concluded that renewal of this deep water occurs between November and

April; however, more recent research by Hooge and Hooge (2002) suggests renewal of the bottom waters can occur at any time during the year.

All tidewater glaciers within the bay except one are currently retreating at some of the fastest rates on Earth (Lawson, 2004). Despite the implications of this increased melt volume for the biogeochemistry of the bay there have been very few studies that have focused on glacial discharge rates. Hill et al. (2009) presented discharge estimates by using regression equations for the south-central and southeastern coastal Alaska to estimate freshwater runoff. Limited ADCP data generally support the predictions from these regression equations, and discharge rates were estimated to range from a few hundred to a few thousand $m^3 s^{-1}$ during a typical year. However, peak discharge can be exceptionally higher, and is estimated to be around 10,000 $m^3 s^{-1}$ to 15,000 $m^3 s^{-1}$ for a 10-year flow event, with broad peak during the summer season, primarily a result of increased precipitation and seasonal snow/ice melt (Hill et al., 2009). This freshwater discharge is the primary control of spatial and temporal changes in salinity and stratification (Etherington et al., 2007). The two arms of the bay are particularly dominated by cold freshwater/glacial runoff from the alpine and tidewater glaciers along their lengths.

In comparison to similar Alaska fjords, GLBA maintains relatively elevated concentrations of phytoplankton throughout the year (Hooge and Hooge, 2002), with the highest standing stocks occurring in summer and lowest during winter when light becomes limited. Hooge and Hooge (2002) observed that within GLBA there was neither a steep drop in the standing stock following the initial spring bloom, nor a suppression of high phytoplankton biomass in fall. The CB consistently has the highest phytoplankton standing stock (Hooge and Hooge, 2002), but Etherington, et al. (2007) found that the regions (LB, CB, EA and WA) with the highest chlorophyll *a* levels varied by season. While there is minimal published literature regarding the composition of the lower trophic levels in GLBA, Renner et al. (2012) identified several middle and upper trophic level organisms, including euphausiids, pink salmon, walleye pollock, and sea otters, many of whose prey typically consists of calcifying organisms such as pteropods, krill and clams.

2.3 Methods

Water column samples were collected at six depths (2, 10, 30, 50,100 m and near the bottom) at each station throughout the bay (Figure 2.1). Ten oceanographic sampling cruises

took place between July 2011 and July 2012. Seasonal data were calculated by averaging each measured parameter for each depth of every cruise. "Summer" consisted of June, July and August, "fall" included September and October; "winter" was comprised of February and March cruises, and "spring" included the months of April and May.

Conductivity-temperature-depth (CTD) data were collected on downcasts with a Seabird 19-plus system. DIC and TA samples were drawn into 250 mL borosilicate bottles. Samples were fixed with a saturated mercuric chloride solution (200 μl), the bottles sealed, and stored until analysis. High-quality DIC data were attained by using a highly precise (0.02%; 0.4 μmoles kg^{-1}) VINDTA 3C-coulometer system. TA was determined by potentiometric titration with a precision of ~1 μmoles kg^{-1}. To ensure accuracy, DIC and TA were calibrated by routine analysis of seawater certified reference materials (prepared and distributed by Andrew Dickson, UCSD). Stable oxygen isotope ($\delta^{18}O$) samples analyze the ^{18}O:^{16}O isotopic ratios. They were collected in 5 ml vials, sealed with paraffin wax and sent to the Stable Isotope Laboratory at Oregon State University's College of Oceanic and Atmospheric Sciences for analysis and all values are given relative to Vienna-standard mean ocean water (VSMOW).

Stable oxygen isotope analysis was used to differentiate water masses with GLBA. The seawater end member for $\delta^{18}O$ (–0.83 ‰) was taken from the bottom depth (127 m) at station 24 outside of Glacier Bay in Cross Sound during Summer 2011 because it had the highest salinity (32.5) of all samples during the year of sampling. A freshwater 'calved' glacier sample was collected near the base of Margerie Glacier at the head of the west arm and had a $\delta^{18}O = -19.90$ ‰. However, at this latitude, glacial end members are typically closer to –21 ‰ (Bowen and Wilkinson, 2002) and since our glacial sample had the potential for an unknown amount of seawater contamination, a more conservative value of –21.00 ‰ was used as the zero-salinity glacial end member. These end members were used to calculate freshwater percentages (FW%) using the equation, $FW\% = -((\text{Obs. } \delta^{18}O + SWEM)/(FWEM + SWEM))$, where Obs. $\delta^{18}O$ is the $\delta^{18}O$ value observed for that water parcel, SWEM is the seawater $\delta^{18}O$ end member and FWEM is the zero-salinity freshwater $\delta^{18}O$ end member.

Aragonite saturation states were calculated from measured temperature, salinity, pressure, DIC, and TA data using CO2SYS (version 2.0), a program that employs thermodynamic models of Lewis and Wallace (1998) to calculate marine carbonate system parameters. For this study we used K_1 and K_2 constants from Mehrbach et al. (1973) and refit by Dickson and Millero (1987),

$KHSO_2$ values from Dickson (1990), the seawater pH scale, and $[B]_T$ value from Uppström (1974).

Figures were prepared using Ocean Data View (ODV) version 4.5.3 (Schlitzer, 2013). Surface plots were gridded using the VG gridding scale with both X and Y gridding scales set to 75 ‰.

2.4 Results and Discussion

2.4.1 Physics and water mass distributions

2.4.1.1 Seasonal T/S distribution

During the summer occupations, the water column in GLBA, especially within the arms, was highly stratified. The surface waters within each arm exhibited the lowest salinities (~23 to 29 for the summer of 2011 and 2012; Figure 2.2) while having a temperature range of ~4° – 10°C during 2011 and 2012. Water depths greater than 2 m, as well as surface waters outside of the arms exhibited a much smaller range in salinity (~30 to 32) and with temperatures between ~3° and 9°C. During the fall of 2011 a vertical density gradient was still present; however, the surface waters with the lowest salinities had shifted into the lower arms and central bay, except for the northernmost station in each arm, which still had low salinity. The two stations at the heads of the arms were likely still impacted by glacial processes such as calving and iceberg melt; however, glacial melt slows during fall and increased winds had likely transported the surface freshwater signal down bay. In winter, the entire water column was well mixed, with temperatures between ~2.5 to 6°C and salinities between ~29 and 32 (Figure 2.2). As solar radiation and glacial melt intensified during spring, the surface waters within the arms of the bay began to increase in temperature and decrease in salinity.

2.4.1.2 Water column fractionation

Samples for $\delta^{18}O$ were used to differentiate water masses within GLBA to determine the relative contribution of freshwater and marine source waters. During the summers of 2011 and 2012, the surface waters exhibited the lowest (most negative) $\delta^{18}O$ values (Figure 2.2), with minimum values at stations near the head of either arm (–9.02 ‰ and –8.23 ‰ in the east arm; –8.46 ‰ and –7.49 ‰ in the west arm). This low $\delta^{18}O$ value from the glacial freshwater was detected within the surface waters as far south as station 04 in lower–central bay. Across the bay,

below 2 m depth $\delta^{18}O$ values were relatively consistent, ranging between ~–2.0 ‰ and –0.8 ‰. During the summer of 2012, a low $\delta^{18}O$ value was also observed in the surface layer, similar to the summer before. However, in 2012, $\delta^{18}O$ values in the upper arms were less negative than the previous summer. Station 18 in the east arm had the lowest $\delta^{18}O$ value (–7.52 ‰) followed by station 12 near the head of the west arm (–7. 39 ‰). During the summer of 2012, the low $\delta^{18}O$ value was observed as far south as station 03, the northernmost station in lower bay. In contrast to 2011, several stations exhibited slightly freshened waters at 10 m, including station 03. Below 10 m, $\delta^{18}O$ values range between ~ –1.0 ‰ and ~ –2.0 ‰. One reason for this could be the result of a deeper mixed layer during the summer of 2012 that was not present in 2011. At station 03, the mixed layer depth (MLD) during the summer of 2011 was ~30 m, while at this station in 2012 MLD was ~50 m. During summer 2011, the maximum isohaline (salinity = 31) intercepted the surface just south of station 03, allowing waters through most of lower bay and outside the sill to mix to depth (up to ~130 m), creating a front and shoaling the mixed layer depth through central bay. Additionally, the summer of 2012 had a stronger freshwater signal in the surface waters along the arms of the bay and into lower-central bay, possibly a result of a higher glacial discharge during this summer as compared to the previous year, though we cannot quantify the specific rates.

Throughout the fall of 2011, low $\delta^{18}O$ waters were still present in the surface layer (Figure 2.2), as well as at 10 m depth within the arms. This surface signal was observed within the arms and continued south through station 03, with station 12 exhibiting the lowest $\delta^{18}O$ value (–5.25 ‰). Below 30 m, as well as through entire water column at stations in lower bay, $\delta^{18}O$ values became relatively uniform and ranged from ~ –2.0 ‰ to –1.4 ‰ (Figure 2.2).

During winter the entire bay was well mixed with a range of $\delta^{18}O$ values between ~ –2.3 ‰ to 1.2 ‰, except for the surface waters at stations 19 and 21 where $\delta^{18}O$ values were –2.57 ‰ and –3.37 ‰, respectively (Figure 2.2). It is likely that the tidewater glaciers at the heads of each arm had continued to influence these stations. Although glacial melt had essentially stopped for the season, the impact of glacial freshwater may have been sustained through calving or iceberg melt. In spring, as temperatures began to increase, the surface waters at stations 12 and 20, the northernmost station in each arm, began to show a lower $\delta^{18}O$ value. $\delta^{18}O$ in surface water at station 12 was –3.13 ‰ and –2.63 ‰ at station 21. Aside from these two surface samples, $\delta^{18}O$ values ranged –2.43 ‰ to –1.25 ‰ (Figure 2.2).

2.5 Spatial and temporal distribution of carbonate parameters

2.5.1 Dissolved inorganic carbon (DIC)

DIC plays a crucial role in influencing seasonal carbonate mineral saturation states through processes such as air–sea gas exchange and primary production. Figure 2.3 shows the relationship between salinity and DIC with a seasonal progression from summer of 2011 (Figure 2.3a) through summer of 2012 (Figure 2.3e). Two distinct water masses were observed during both summer seasons, with higher salinity and DIC concentrations in waters from the middle and lower bay, as well as samples taken from below the surface layer within the arms, while lower salinity and DIC concentrations were present near the surface at stations within the two arms and the north-central bay.

Figure 2.4 (top row) depicts the seasonal DIC distribution in only the surface waters (top 2 m) across the bay from summer 2011 through summer 2012. In summer 2011, DIC concentrations in the surface waters varied from 1273 (station 19) to 2044 μmoles kg^{-1} (station 02), while surface water DIC during summer 2012 ranged from 1502 (station 18) to 2001 μmoles kg^{-1} (station 24). These low DIC concentrations were partially due to primary productivity that consumed DIC in the euphotic zone, while low-DIC glacial runoff diluted concentrations at the surface. Strong summer stratification set up by both temperature and density gradients also inhibited vertical mixing of DIC and nutrient-rich water from mixing up to the surface within the arms of the bay. However, Hooge and Hooge (2002) speculated that tidally induced internal waves (Matthews, 1981) coupled with proposed hydraulic instabilities that result from GLBA's high currents and constriction over the entrance sill help nutrients diffuse upward without disrupting stratification. They suggest this as one possible explanation for the sustained productivity observed throughout the summer season, though a more biologically-based study is needed in this area.

As temperatures decreased and wind mixing increased in the fall, DIC concentrations in the surface waters increased slightly, primarily in the arms and upper-central bay. In the lower bay, DIC concentrations remained relatively consistent between summer and fall 2011 with fall concentrations between 1700 and 2043 μmoles kg^{-1}. During winter, the water column throughout the bay was fairly homogenous, likely a result of wind mixing and the breakdown of density-driven stratification as glacial melt halted for the year. Winter DIC concentrations were between

1911 μmoles kg^{-1} and 2071 μmoles kg^{-1}. Between winter and spring, DIC concentrations decreased, especially within the arms. The seasonal surface DIC concentrations during the spring 2012 varied from 1753 μmoles kg^{-1} (station 20) to 2026 μmoles kg^{-1} (station 01). This drawdown of DIC within the arms may be attributed to the onset of glacial melt in the spring caused by increased solar heating, which strengthens stratification and allows phytoplankton so stay in the euphotic zone, enhancing primary production.

2.5.2 Total alkalinity (TA)

Along with DIC, TA is a second key component of the carbonate system in GLBA. Freshwater, such as glacial melt, is relatively low in TA compared to marine waters, and when this freshwater enters the marine environment it has the potential to reduce the capacity of seawater to buffer against changes in pH. Figure 2.5 depicts the seasonal relationship between salinity and TA in GLBA and shows a similar pattern that was seen in the DIC data. As with DIC, during summer (Figure 2.4 top row) there were two distinct water masses. The first was the high salinity, high TA marine water found in central and lower bay and in the deeper waters within the arms. The second grouping was the lower salinity, lower TA fresh surface waters of the arms. This low TA signal in the surface water was the result of tidewater glacial melt draining into the surface waters along the arms.

Figure 2.4 (second row) shows the seasonal TA distribution in the surface waters across the bay from summer 2011 through summer 2012. During both summer seasons, low TA concentrations were observed in the arms, especially in the most northern region where the tidewater glacier are concentrated. The low TA signal in the upper arms was more intense nearest the heads of the bay during the summer of 2011 than the following summer in 2012. However, during the summer of 2012 the lower TA surface plume extended farther south than in 2011. During summer 2011, TA concentrations in the upper arms were at their lowest observed levels during the first year of sampling with the surface waters at station 20 reduced to 1411 μmoles kg^{-1}. During summer 2012, surface TA ranged from 1412 at station 18 to 2137 μmoles kg^{-1} at station 13.

This low-TA signal subsided between summer and fall as air and surface water temperatures began to decrease, effectively ending seasonal glacial melt. Additionally, increasing wind speeds during this time of year enhanced vertical mixing, breaking down the

strong surface stratification within the arms that summer warming and glacial melt created. Across the middle bay, TA concentrations decreased slightly between summer and fall 2011 as some of the low alkalinity freshwater flowed south out of the arms and into middle bay. In the lower bay, TA concentrations, especially in Cross Sound, increased slightly, likely due to increased wind-driven vertical mixing, and in the case of station 24, direct access to ocean water. Bay-wide, TA concentrations in the surface water during the fall of 2011 varied between 1760 μmoles kg^{-1} at station 12 and 2103 μmoles kg^{-1} at station 01.

TA concentrations continued to increase between fall of 2011 and winter of 2012 at all locations in the bay (Figure 2.4). During winter months, the bay waters became fairly well mixed, with slightly higher TA concentrations in the lower bay than within the arms. The transition from winter to spring typically consists of increasing atmospheric temperatures and solar radiation, which restarts the glacial melt process. This melting reintroduces fresh glacial runoff into the arms lowering the TA concentrations in the upper arms, especially within the west arm (Figure 2.4). The central bay and the east arm saw little change in TA concentrations between the winter and spring occupations. This may be due to the fact that there are fewer tidewater glaciers along the east arm than the west arm and the glacial melt had not increased enough to impact surface waters within the east arm, while the northernmost portions of the west arm were already being affected by the impact of freshwater input.

2.5.3 Aragonite saturation state (Ω_A)

The saturation states of carbonate minerals throughout the bay are largely controlled by the dynamic changes in DIC and TA concentrations and to a smaller extent salinity and temperature. Figure 2.6 shows the seasonal trends of aragonite saturation state with depth. The data clearly show that during summer there was a wide range of saturation states, especially in the surface waters, with some of the lower salinity surface samples falling below the saturation horizon where $\Omega = 1$. In the summer of 2011, aragonite saturation states (Ω_A) ranged from 0.39 in the surface waters at station 20 and 2.91 at station 04 at depth of 20 m, while in the summer of 2012 Ω_A had a much larger range from 0.13 at the surface of station 18 to 3.51 at station 08 at 10 m. The low salinity, undersaturated samples at the surface in Figure 2.6a and 2.6e are from the stations within the arms where fresh glacial melt sits atop the denser, more marine waters during the melt season. These low Ω_A in the arms can also be seen in the seasonal surface plots in Figure

2.4 (third row). During summer, temperatures and solar radiation are at a maximum, thus increasing glacial runoff into the marine waters and reducing TA and saturation states, but the reduction in Ω is somewhat buffered by the removal of DIC from primary production. This balance between DIC and TA plays out through the entire year and ultimately determines whether or not aragonite undersaturations occur.

Between the summer and fall of 2011, Ω_A dropped across the surface waters of the bay. In fact, all surface waters within the bay had become undersaturated with respect to aragonite in the fall months. This is clearly seen in Figure 2.4, where purple colors represent $\Omega < 1$. Samples taken from depths below this surface layer (2 m depth) were near $\Omega = 1$. This bay-wide surface undersaturation may be the result of increasing wind speeds mixing the low TA glacial water into the lower bay.

Winter Ω_A values (Figure 2.6c) ranged from 0.55 (station 02, 20 m) to 2.74 (station 10, 100 m) and surface waters had the widest range of values of Ω_A. Figure 2.4 shows that in winter, despite strong wind mixing and lack of glacial melt in the surface layer, there were still patches of aragonite undersaturation, including the northern tips of each arm and in Cross Sound. The undersaturations at the northern end of each arm may have been due to marine waters being in constant contact with tidewater glacier faces and that, even though there is no active melting from solar radiation, there is glacier calving and melting of icebergs within the marine waters. Furthermore, there can be direct ablation at the glacier-seawater interface as a result of above-freezing marine water directly melting the glacier face.

Figure 2.6d shows that during spring of 2012 almost all samples, including all surface samples (Figure 2.4), were supersaturated with respect to aragonite. Aragonite saturation states varied between 0.90 (station 16 at 284 m) and 3.26 (station 20, surface), while surface Ω_A ranged between 1.21 (station 24) and 3.26 (station 20). This increase in Ω_A, especially at the surface, can be attributed to the spring onset of primary production, which consumes DIC in the mixed layer, thus increasing Ω_A in these waters.

2.6 Controls on aragonite saturation states

Figure 2.4 (bottom row) shows the seasonal percentage of freshwater in the upper 2 m across the bay from the summer of 2011 through the summer 2012. These surface plots

demonstrate that during the summer seasons, the surface waters in the arms of the bay were as much as ~40% freshwater, while during the winter freshwater percentage was < ~10%.

The role of freshwater in the bay can be seen in Figure 2.7, which illustrates the relationship between freshwater percentage, TA, and Ω_A and includes all surface samples taken during cruises between the summer of 2011 and summer of 2012. This relationship demonstrates that water with a higher percentage of freshwater also has lower TA concentrations, thus leading to low Ω_A. It is this relationship that supports our contention that freshwater from tidewater glacier discharge leads to undersaturations due to the low TA concentrations and reduced buffering capacity. The points at high TA concentrations and low percent freshwater (Figure 2.7) are from the surface waters of stations outside of the bay's entrance sill, as well as those from the lower bay. Conversely, the points with low TA concentrations and high freshwater content were found at stations within the arms of the bay and represent the locations that are most strongly influenced by glacial runoff.

In order to determine the sensitivity of the carbonate systems to varying parameters we calculated Ω_A for surface waters (2 m depth) at the eight core stations during each season using the thermodynamic models of Lewis and Wallace (1998). To identify the degree to which each variable impacted the seasonal change in Ω_A, at each station, Ω_A was recalculated by adjusting only one variable at a time while keeping the remaining variables (temperature, salinity, etc.) consistent with measured values. For example, we calculated the observed change in Ω_A between the summer and fall of 2011 and then recalculated the carbonate parameters using the DIC measurement from the fall while keeping the remaining variables as those measured during the summer. By doing this, we were able to identify the one-dimensional impact that DIC alone would have had on the change to Ω_A between these two seasons. By repeating these calculations for each of the most influential parameters (TA, temperature, salinity, and the combination of DIC and TA), we were able to identify the degree by which each parameter impacted the carbonate system. We found that there were very minimal changes in seasonal Ω_A due to differences in temperature and salinity, but found that the combination of DIC and TA was responsible for most of the changes to Ω_A. However, we also determined that the dominant controls on Ω_A varied both seasonally and spatially within the bay.

2.6.1 Seasonal and spatial changes in Ω_A

Table 2.1 shows the impact of DIC, TA, and salinity on surface Ω_A at the eight core stations in GLBA between each season. As expected, there was little to no impact on Ω_A due to changes in salinity alone as this can be seen at all stations throughout the duration of the study. The data clearly show that DIC and TA were the primary factors in modifying Ω_A in GLBA, though the magnitude of their influence varied seasonally.

For example, during the transition from summer to fall in 2011 there was some correlation between the direction of change in Ω_A and a station's latitudinal location. Stations 12 and 20 at the northern ends of the arms had an increase in DIC and TA, while stations 07 and 16 halfway down the arms showed an increase in DIC and a decrease in TA. However, the primary controls behind the changes to Ω_A in the surface water had less correlation. In the west arm, Ω_A decreased at both stations 12 and 07. At station 12, this change was due to an increase in DIC, while at station 07, TA was the main control on Ω_A, possibly the result of low-TA glacial melt flowing south as cooling temperatures slowed glacial melt. Within the east arm, there is one glacier that is tidewater at all tidal stages and one glacier that is tidewater only at extreme high tides (Sharman, 2010). These can cause differences in the influences on TA among stations in this region. For example, TA at station 16 was directly affected by the glacial outflow of meltwater from glaciers up-bay from its location, while only one glacier at the head of the arm directly affected TA at station 20. While there are more tidewater glaciers in the west arm, they are all located north of station 07 and tend to influence TA at the stations in a similar way as in the east arm. These spatial differences between the upper arm stations (12 and 20) and the mid-arm stations (07 and 16) may have been due to increasing winds in fall pushing the low-TA summer glacial melt southward. Additionally, cooling temperatures during fall slowed glacial runoff, likely allowing TA concentrations at the ends of the arms to increase.

As a result of cooling between fall and winter, a decrease in glacial/freshwater runoff and increasing winds broke down stratification allowing vertical mixing of TA- and DIC-rich water from depth. Increased winds also enhance air–sea gas exchange within the surface waters. While this mixing brought more DIC-rich water from depth and aided gas exchange, the increases in TA were large enough within the arms and upper-central bay to counteract the increases in surface water DIC, and the observed Ω_A increased as a result (Table 2.1). As with station 13 and those stations within the arms, DIC and TA concentrations increased in the lower-

central bay between fall and winter. However, at station 04 there was a slight decrease in Ω_A, suggesting that the increase in DIC had a larger effect on these surface waters than the increased TA. In the lower bay, at station 01, a small increase in TA counteracted a very small increase in DIC to cause a net increase in Ω_A. Station 24 experienced a very small decrease in Ω_A between fall and winter, with increasing DIC concentrations accounting for the net change in Ω_A.

During the transition from winter to spring in 2012, DIC played a larger role than TA in changing Ω_A at many stations. Within both arms where TA was the main control between fall and winter, DIC took over as a dominant influence going into spring. At the head of the west arm, DIC was the primary influence on Ω_A at station 12. Despite the onset of the glacial melt season, warming temperatures, an increasing number of daylight hours, and enhanced stratification allowed for an increase in primary production, thus decreasing DIC concentrations in the surface waters and raising Ω_A. Farther south at station 07, a combination of increasing TA and decreasing DIC concentrations caused a net increase in Ω_A. Within the east arm TA played a minimal role in changes to surface Ω_A, having almost no impact on the change in Ω_A at either of these stations. At station 20, a drawdown of DIC (~245 μmoles kg^{-1}) had a large influence on surface Ω_A, which caused a net increase in Ω_A of more than two units. This may have been the result of a spring phytoplankton bloom. Inorganic nutrient concentrations at this station were low, but comparable values were observed at the northernmost station within the west arm. The onset of glacial melt helps to establish stratification within the arms and can act to enhance primary production. However, the exact mechanism for the large DIC drawdown at station 20 cannot be confirmed at this time.

At station 16, the impact of DIC and TA on changes to Ω_A were very similar to those of station 20; however, the magnitude of impact at station 16 was less than half that of station 20. Both of the stations in the lower bay experienced a drawdown of DIC in the surface water, most likely due to increased primary production. However, station 24 had a decrease in surface TA, while TA concentrations at station 01 increased slightly, by ~13 μmoles kg^{-1}. This may be the result of differential mixing due to the location of each station. Station 01 lies within the bay just past the entrance sill and station 24 is outside of the bay in Cross Sound. Although net Ω_A increased at both stations by roughly the same amount, the increase in Ω_A at station 24 was most influenced by elevated DIC while at station 01 Ω_A increased as a result of both, DIC drawdown and increased TA.

Between spring and summer, a similar, yet opposite pattern emerged within the arms than was seen between fall and winter. During this seasonal transition, temperatures and glacial runoff were increasing, causing surface TA concentrations at stations nearest the tidewater glacier outflows to decrease. DIC concentrations in the surface waters decreased within the arms, as well as across the bay at all stations except station 24 in Cross Sound, likely due to high rates of primary production. Although decreasing concentrations of DIC typically act to increase the Ω_A, the influx of low-TA melt water at these stations overrode this process and we observed decreasing Ω_A. At all stations within the two arms DIC, TA and Ω_A decreased in the surface waters. The increased flux of low TA glacial meltwater caused surface Ω_A to decrease, despite the relatively large drawdown of DIC via primary production. At the stations within the central bay, DIC became the primary control on Ω_A. At station 13, however, an increase in TA helped to increase Ω_A in these waters. Throughout the lower bay, net changes to Ω_A were relatively small (< 0.2), with DIC controlling Ω_A at station 01 and TA controlling Ω_A at station 24. The difference in the control mechanisms in the lower bay are not fully understood at this time, but may be due to tidal interactions and circulation patterns across the entrance sill of the bay, as well as in Cross Sound and Icy Strait.

2.7 Potential impacts of anthropogenic CO_2 in GLBA

The uptake of anthropogenic CO_2 into the surface oceans has already lowered the average ocean pH by ~0.1 units, with a continued reduction of 0.1 to 0.5 units expected in the next ~100 years (Caldeira and Wickett, 2003; Feely et al., 2004; Orr et al., 2005). While most OA research to date has been done for the open ocean, few studies have focused on estuarine ecosystems. Unique coastal processes that among other things reduce salinity and alkalinity concentrations and dampen the buffering capacity of these waters, making them more susceptible to changes in pH than the open ocean (Miller et al., 2009), although these regions naturally have seasonally varying pH values that may exceed current anthropogenic impacts.

While we cannot directly quantify the anthropogenic CO_2 inventory in GLBA, the effects of it can be estimated. Sabine et al. (2004) estimated that ~50 μmoles kg^{-1} of anthropogenic CO_2 has entered the surface waters of the North Pacific Ocean. Although the North Pacific acts as oceanic source water to GLBA, the surface waters within the bay are highly influenced by large volumes of low alkalinity glacial melt. Therefore, a more conservative estimate of ~45 μmoles

kg^{-1} of DIC was used as a basis for the surface water anthropogenic CO_2 inventory. To estimate the effects of anthropogenic CO_2 on OA in the bay, ~45 μmoles kg^{-1} were removed from the measured DIC values while all remaining variables remained as observed, representing preindustrial conditions (Mathis et al., 2011b, Mathis and Questel, 2013). Saturation states were then recalculated using the Lewis and Wallace (1998) thermodynamic model. When this was done for each season in GLBA, almost all of the undersaturated samples became supersaturated with respect to aragonite. During both summer seasons, the only samples that remained undersaturated after removing the anthropogenic signal were those of surface waters within the arms of the bay. A similar pattern was seen in winter, when all waters became supersaturated with the exception of one subsurface sample. During the fall, all surface waters, as well as several samples from depths below 2 m, were undersaturated. However, upon removal of the anthropogenic CO_2 signal, all of the fall samples became supersaturated.

This simple approximation demonstrates the impact that anthropogenic CO_2 has on marine systems such as GLBA. As atmospheric CO_2 concentrations continue to rise, this anthropogenic signal, in both the atmosphere and seawater, will also increase. Wanninkhof et al. (2013) showed that the partial pressure of CO_2 (pCO_2) is increasing in the North Pacific by ~1.5 ppm yr^{-1} or ~75 ppm every 50 years. Using this rate of increasing pCO_2 along with data from our discrete measurements, we found that in 50 years Ω_A will decrease by an average of 0.16 across the bay, with the largest effects seen during the spring season (average $\Delta\Omega_A = 0.36$). We also found that if current CO_2 trends continue at this rate, the surface waters of the bay will become perennially undersaturated in aragonite in ~150 years (Table 2.2). However, because the rate of CO_2 accumulation is also increasing, it is likely that this is a conservative estimate and does not take into account the increase in pCO_2 due to rising water temperatures in the bay. Additionally, this estimate does not include potential acidifying affects of increased freshwater and glacial inputs, which will also increase pCO_2, and lower TA concentrations compared to pre-industrial values.

Both the current and predicted future changes in the carbonate chemistry of GLBA will likely have an impact on its biology. During a 2008 study on live pteropods (*Limacina helicina antarctica)* extracted from the Southern Ocean, Bednarŝek et al. (2012) observed rapid dissolution of aragonitic shells within eight days of incubations in seawater with Ω_A between 0.94 and 1.12. This suggests that rapid or severe dissolution of aragonitic shells can occur when

Ω_A is near the saturation horizon (Ω_A = 1). This could have major repercussions on systems such as GLBA where surface waters already exhibit seasonal undersaturations that can last for several months. GLBA has large populations of calcifying organisms including barnacles, mussels, sea stars (Milner et al., 2007) and krill, which act as a vital link between phytoplankton and higher trophic levels such as humpback whales, as well as a variety of commercial shellfish and crab species. While it is currently unknown what specific niche pteropods occupy in the GLBA ecosystem, they can be an important prey source for juvenile pink salmon and other pelagic fish. However, their main benefit could be that of an indicator species, the proverbial "canary in the coalmine", that provides early insights into species sensitivities and vulnerabilities as environmental conditions change in the coming decades.

2.8 Conclusions

Over the past two centuries, GLBA has experienced rapid deglaciation of its numerous terrestrial and tidewater glaciers leading to an increase in the amount of freshwater entering the marine ecosystem. This deluge of low-TA freshwater has likely reduced the buffering capacity of surface waters and enhanced the estuary's vulnerability to further changes in pH, contributing to seasonally enhanced reductions in biologically-important carbonate minerals.

Our data have shown that GLBA experiences seasonal aragonite undersaturation events that vary in intensity and extent throughout the year. While increased CO_2 emissions and uptake by ocean surface waters are typically thought to be the major cause of OA in marine systems, this is only part of the story in GLBA. We identified the primary influences of surface Ω_A and found them to vary spatially and seasonally. DIC concentrations drove changes in Ω_A in the lower bay, as well as seasonally within the arms during the highly productive spring and summer months. However, TA concentrations were the major influence within the arms from spring through fall, when glacial discharge rates were the highest. GLBA receives glacial input from both tidewater and alpine glaciers, though the arms of the bay are highly impacted by tidewater glacier melt, which discharge directly into the marine system via calving, iceberg melt, and direct melting of the glacier faces. As a result of this low-TA glacial runoff, we observed the lowest Ω_A (0.40) at the head of the east arm during the summer of 2011. The fact that GLBA has a number of tidewater glaciers along its upper arms, rather than solely alpine glaciers, may play an important role in controlling the abundance of carbonate minerals in the bay. Tidewater

glaciers discharge low TA freshwater directly from the glacier face into the marine waters. This discharge does not pass over terrestrial materials as outflow streams from alpine glaciers do. As alpine glacier melt streams flow across land they react with the carbonate bedrock, increasing the concentration of TA prior to entering the marine environment (Brown, 2002).

The data collected during this study showed that surface waters in GLBA with the highest percentage of freshwater directly corresponded with areas of aragonite undersaturation or near-undersaturation. This effect was most notable within the two arms during the peak glacial melt season, but can affect the bay as a whole. For instance, during the fall of 2011, we observed that all surface waters in the bay were undersaturated with respect to aragonite, likely the result of winds and tidal currents driving the low TA freshwater out of the arms and south towards the bay's entrance. Glacial melt then stopped and surface Ω_A increased across the bay during the winter as a result of cooling temperatures, stratification breakdown and tidal mixing.

As glacial melting rates continue to increase in tandem with warming global temperatures, GLBA will likely see enhanced carbonate mineral undersaturation events that will exacerbate the CO_2-drive OA process. The combination of these two drivers will likely increase the extent, duration and intensity of carbonate mineral undersaturations with detrimental, yet currently unknown effects to the diverse biological food web in the bay. However, TA-driven reduction in Ω is not unique to GLBA and is likely a prominent feature in coastal areas that receive high volumes of runoff from tidewater glaciers, both in Alaska and around the World. This is certainly the case throughout the northern and eastern Gulf of Alaska, stretching from British Columbia to the Aleutian Islands and may be even more prevalent around Greenland, where glacial discharge is orders of magnitude higher than in our study region. This non-CO_2 driven reduction in carbonate mineral saturation states certainly warrants more extensive study as it is yet another potential stressor to vulnerable marine ecosystems.

2.9 Figures

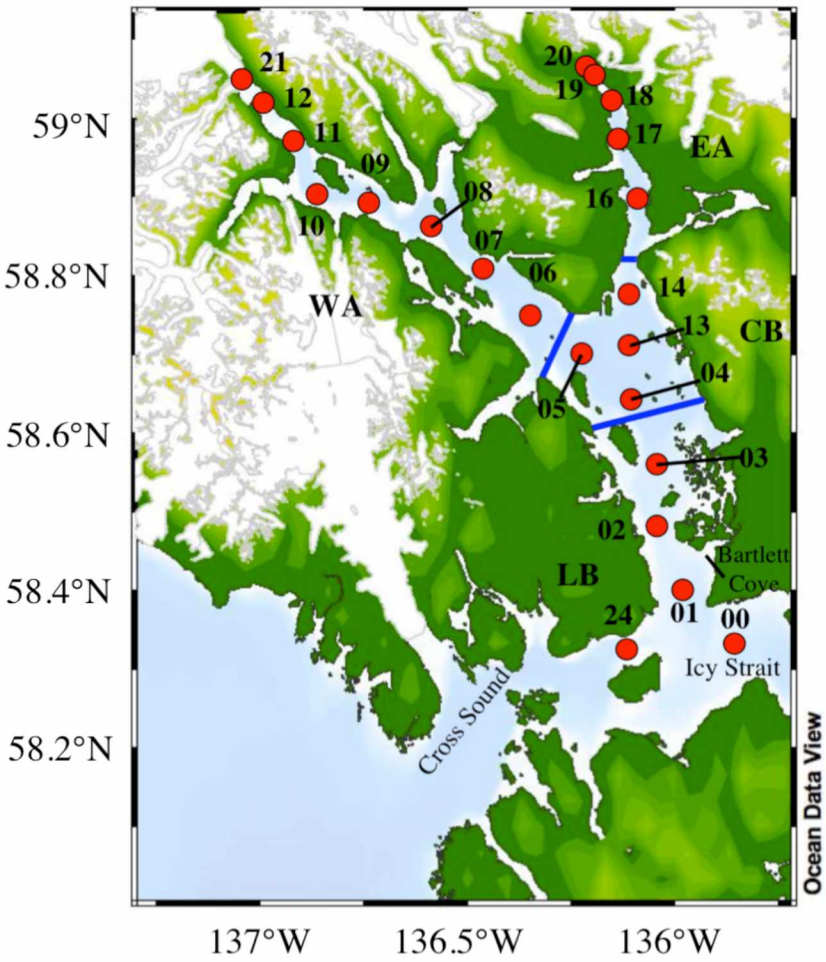

Figure 2.1 — GLBA sampling location map: Map of southern Alaska and Alaska panhandle. Inset shows the marine waters of Glacier Bay National Park and Preserve with oceanographic sampling stations marked.

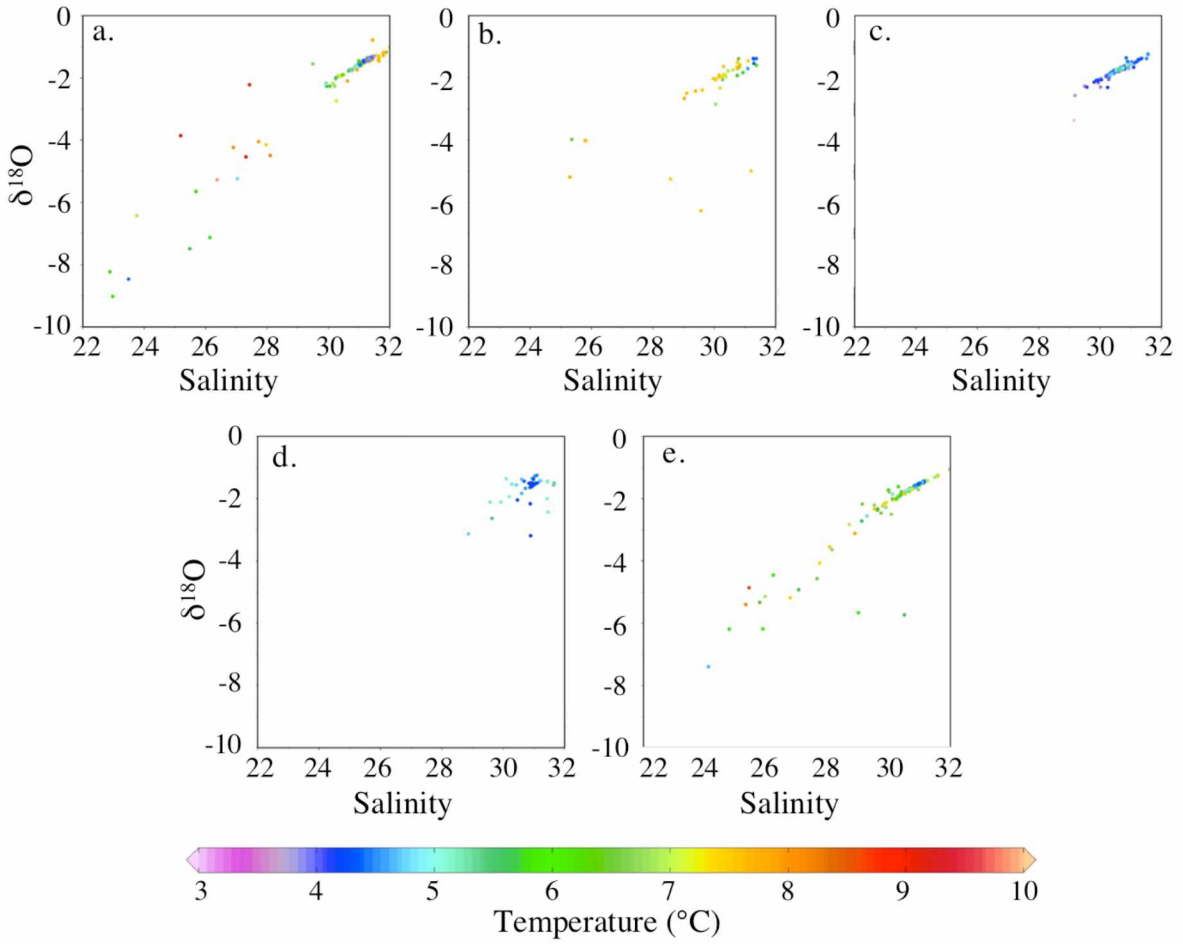

Figure 2.2 — Salinity vs. $\delta^{18}O$ (‰): Seasonal surface plots of salinity vs. $\delta^{18}O$ from summer 2011 a.) summer 2011, b.) fall 2011, c.) winter 2012, d.) spring 2012, e.) summer 2011. Color bar represents temperature in °C.

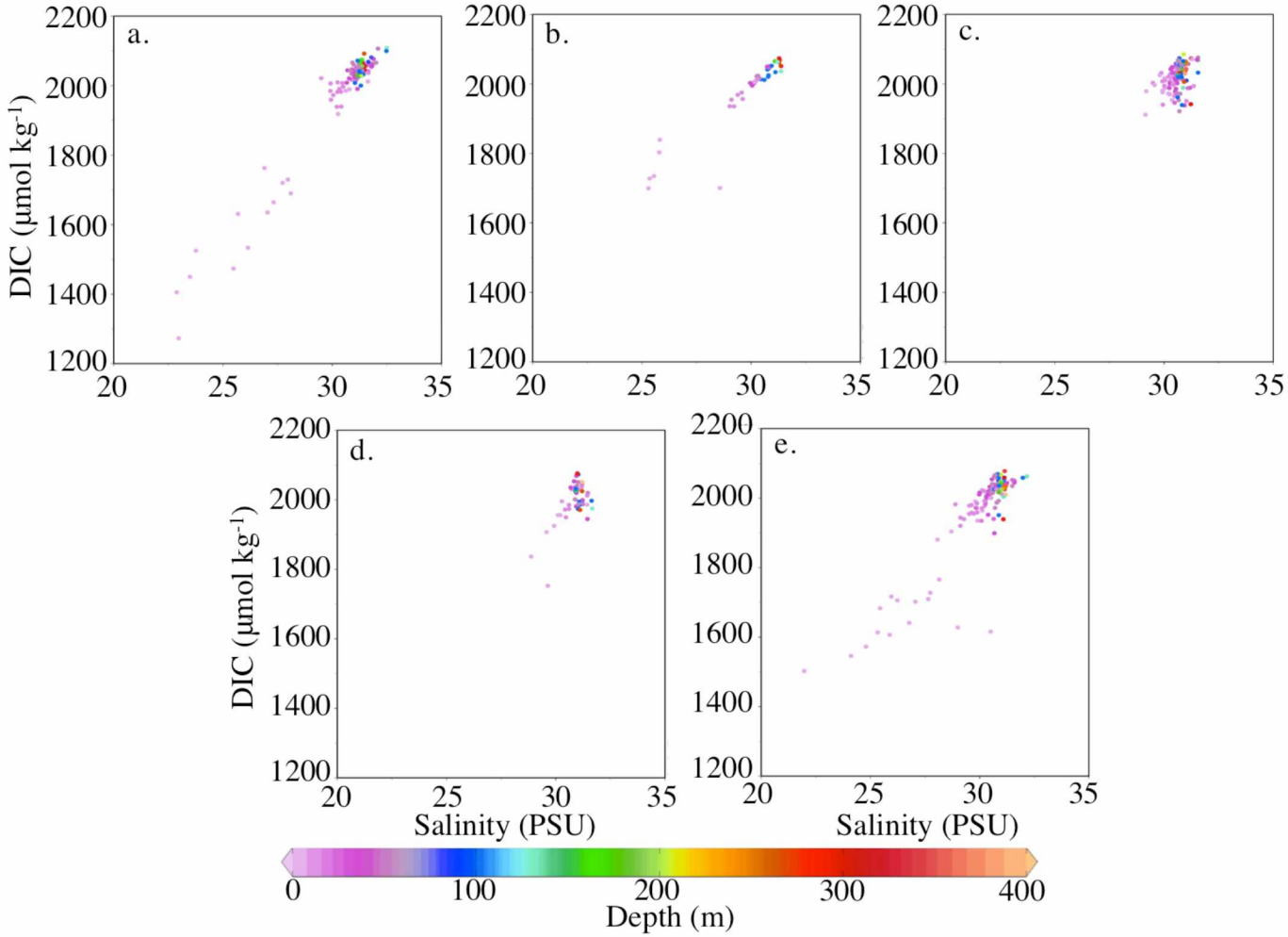

Figure 2.3 — Salinity vs. dissolved inorganic carbon: Seasonal scatter plots of salinity vs. DIC from summer 2011 a.) summer 2011, b.) fall 2011, c.) winter 2012, d.) spring 2012, e.) summer 2011. Color bar represents depth.

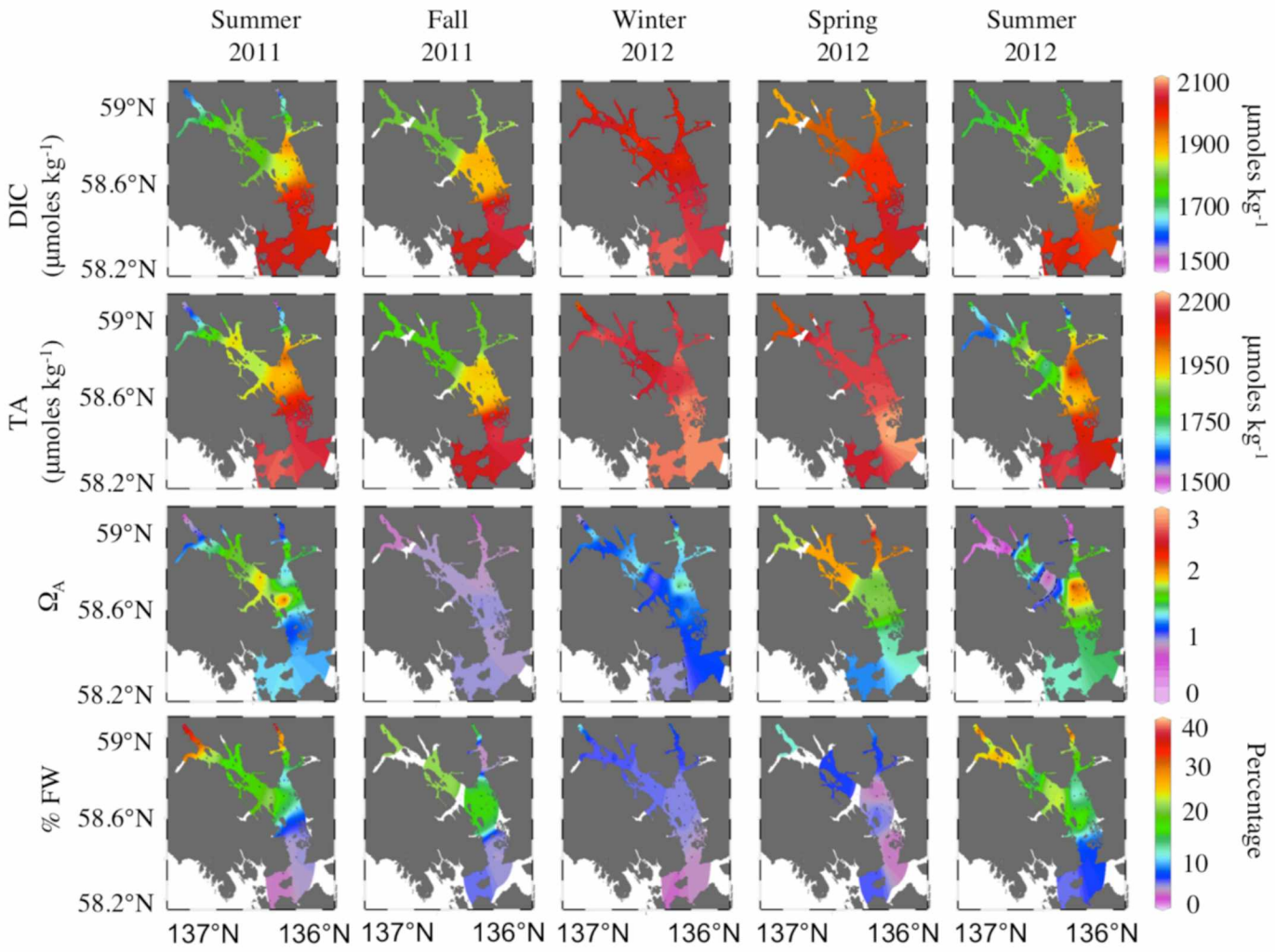

Figure 2.4 — Seasonal surface plots: Seasonal DIC (top row), TA, Ω_A, and %FW (bottom row) in the surface layer from summer 2011 (left) fall 2011, winter 2012, spring 2012, summer 2012 (right)

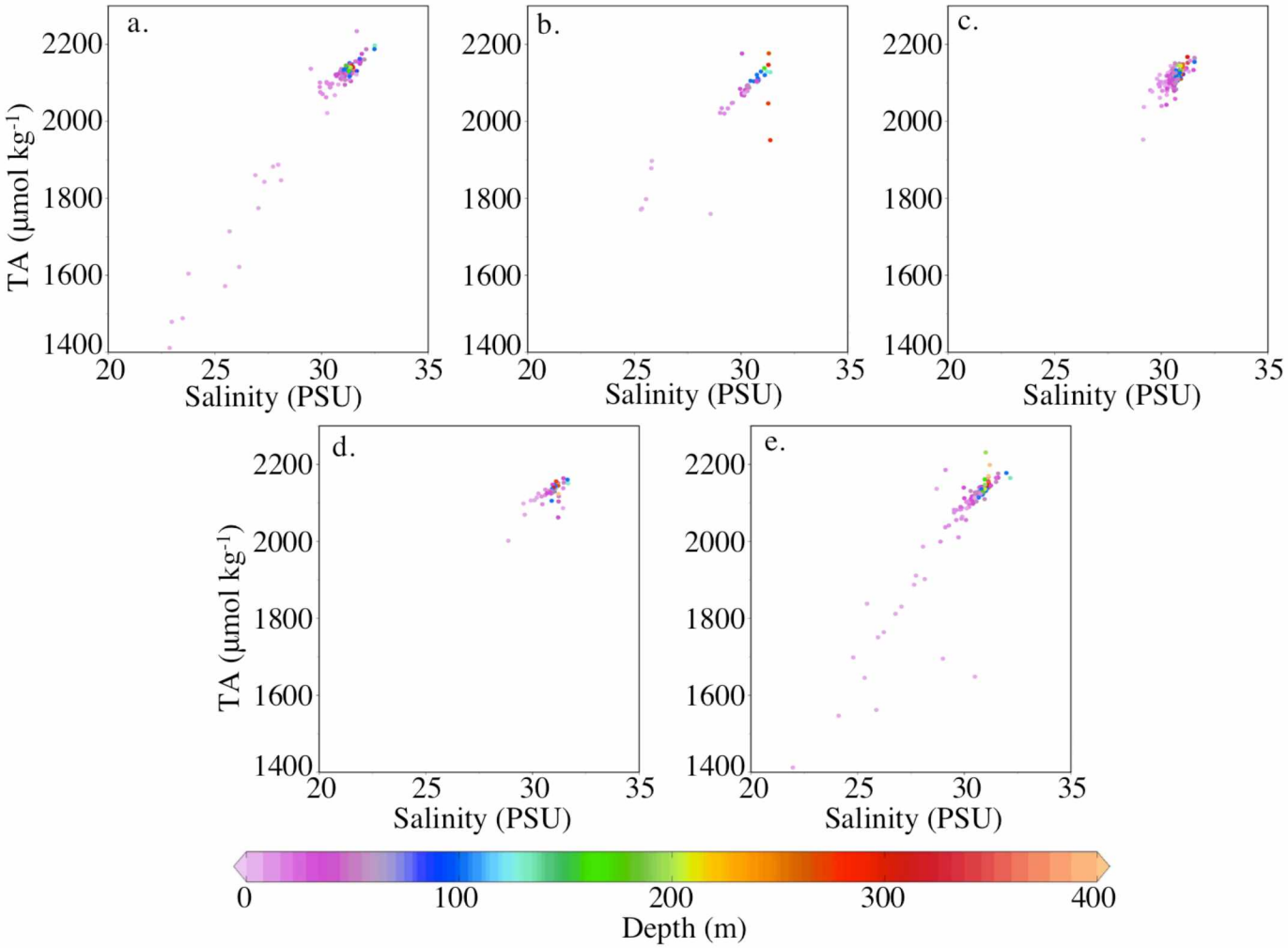

Figure 2.5 — Salinity vs. total alkalinity: Seasonal scatter plots of salinity vs. TA from summer 2011 a.) summer 2011, b.) fall 2011, c.) winter 2012, d.) spring 2012, e.) summer 2012. Color bar represents depth.

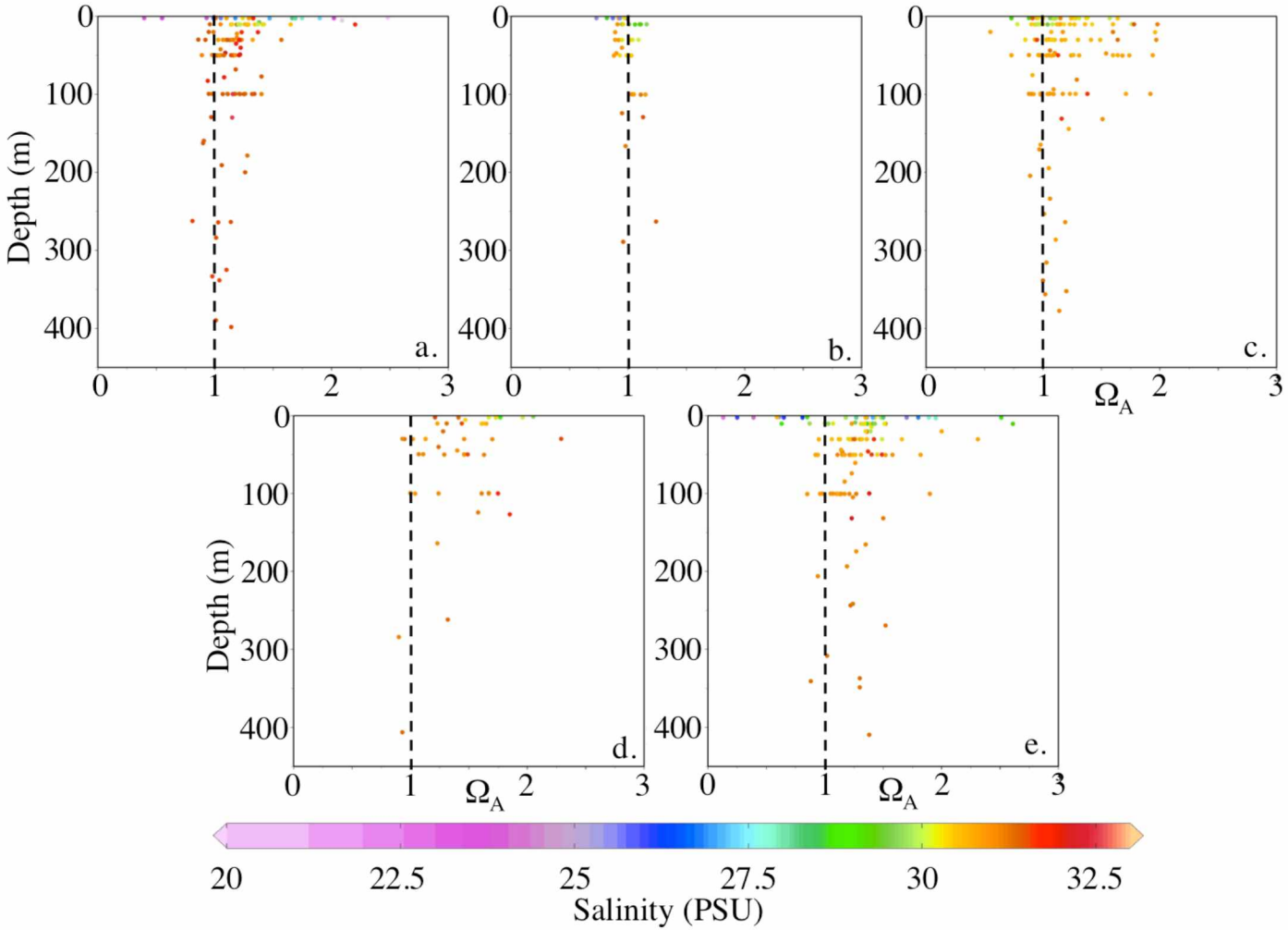

Figure 2.6 — Salinity vs. aragonite saturation state: Seasonal scatter plots of salinity vs. Ω_A from a.) summer 2011, b.) fall 2011, c.) winter 2012, d.) spring 2012, e.) summer 2012.

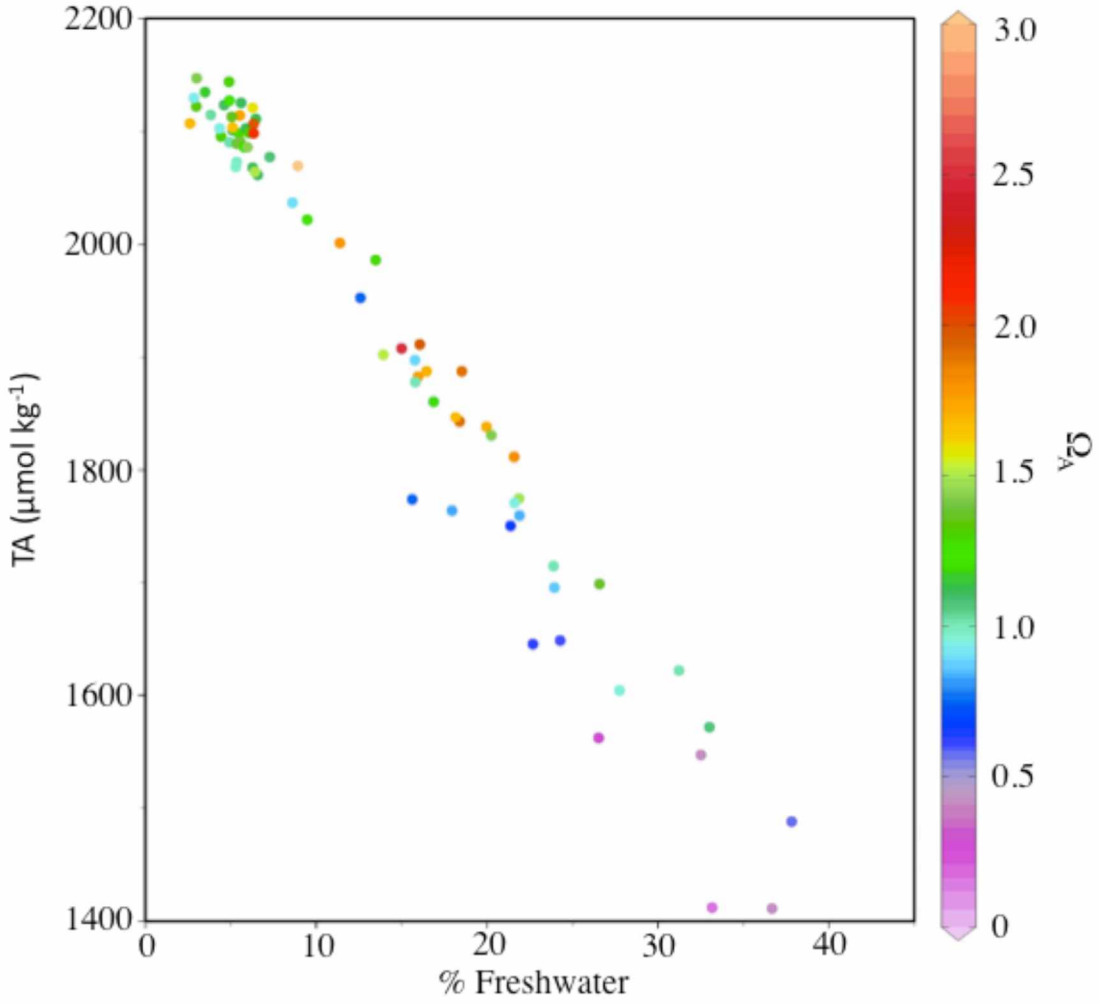

Figure 2.7 — Freshwater vs. total alkalinity: Scatter plot of percentage of FW present vs. TA with aragonite saturation state represented with the color bar. This figure shows that waters with higher freshwater percentage are low in TA and correspond with lower aragonite saturation states.

2.10 Tables

Table 2.1 — Controls on seasonal changes to aragonite saturation state: Table showing the actual change to Ω_A between seasons, $\Delta\Omega_A$ as a result of changes in salinity, and the $\Delta\Omega_A$ as a result of changes in, both, DIC and TA simultaneously at each station.

Controls on Seasonal Changes to Aragonite Saturation State

Seasons	Station	$\Delta\Omega_A$ Sum '11 – Fall '11	$\Delta\Omega_A$ Fall '11 – Win '12	$\Delta\Omega_A$ Win '12– Spr '12	$\Delta\Omega_A$ Spr '12 – Sum '12
Observed Change	1	–0.37	0.22	0.26	0.07
Change due to DIC	1	–0.41	–0.01	0.15	0.83
Change due to TA	1	0.06	0.25	0.10	–0.65
Change due to Salinity	1	0.00	0.00	0.00	0.01
Observed Change	4	–1.39	0.00	0.74	0.22
Change due to DIC	4	–1.01	–0.82	0.50	2.23
Change due to TA	4	–0.34	2.13	0.19	–1.40
Change due to Salinity	4	–0.24	–0.02	0.00	0.03
Observed Change	7	–0.75	0.44	0.59	–0.46
Change due to DIC	7	–0.09	–0.81	0.39	1.55
Change due to TA	7	–0.68	3.30	0.15	–1.55
Change due to Salinity	7	0.04	–0.02	0.00	0.03
Observed Change	12	–0.24	0.27	0.68	–1.38
Change due to DIC	12	–0.93	–0.71	1.24	2.87
Change due to TA	12	1.85	2.95	–0.43	–1.71
Change due to Salinity	12	–0.03	–0.01	0.01	0.07
Observed Change	13	–0.30	0.78	0.02	0.84
Change due to DIC	13	–0.56	–0.56	–0.02	0.48
Change due to TA	13	0.34	2.01	0.03	0.29
Change due to Salinity	13	0.01	–0.01	0.00	0.02
Observed Change	16	–0.88	0.44	0.74	–0.16
Change due to DIC	16	–0.13	–0.75	0.72	1.96
Change due to TA	16	–0.77	3.07	–0.01	–1.64
Change due to Salinity	16	0.03	–0.02	0.00	0.03

Table 2.1 continued

Seasons	Station	$\Delta\Omega_A$ Sum '11 – Fall '11	$\Delta\Omega_A$ Fall '11 – Win '12	$\Delta\Omega_A$ Win '12– Spr '12	$\Delta\Omega_A$ Spr '12 – Sum '12
Observed Change	20	0.35	0.33	2.20	–2.45
Change due to DIC	20	–0.33	–0.63	2.27	0.47
Change due to TA	20	3.48	3.03	–0.06	–2.75
Change due to Salinity	20	0.00	–0.01	0.00	0.11
Observed Change	24	–0.35	–0.06	0.30	0.14
Change due to DIC	24	0.05	–0.40	0.68	–0.12
Change due to TA	24	–0.40	0.48	–0.28	0.23
Change due to Salinity	24	0.01	0.00	0.00	0.01

Table 2.2 — Seasonal, preindustrial and projected aragonite saturation states: Current and projected seasonal averages of Ω_A averages of surface waters. Projected Ω_A were calculated assuming 45 μmoles kg^{-1} of anthropogenic CO_2 entering GLBA per year.

Seasonal, Preindustrial and Projected Aragonite Saturation States

Season	Obs. Ω_A	Preind. Ω_A	Ω_A 50 yrs	Ω_A 100 yrs	Ω_A 150 yrs
Summer 2011	1.38 ± 0.59	1.78 ± 0.65	1.13 ± 0.42	0.97 ± 0.33	0.85 ± 0.27
Fall 2011	0.89 ± 0.09	1.25 ± 0.09	0.79 ± 0.08	0.72 ± 0.07	n/a
Winter 2012	1.19 ± 0.24	1.57 ± 0.26	1.04 ± 0.18	0.92 ± 0.14	0.83 ± 0.11
Spring 2012	1.88 ± 0.62	2.30 ± 0.64	1.52 ± 0.38	1.28 ± 0.26	1.11 ± 0.19
Summer 2012	1.51 ± 0.63	1.90 ± 0.68	1.25 ± 0.48	1.07 ± 0.38	0.94 ± 0.32

2.11 References

Arendt, A.A., Echelmeyer, K.A., Harrison, W.D., Lingle, C.S., Valentine, B., 2002. Rapid wastage of Alaska glaciers and their contribution to rising sea level. Science, 297: 382–386.

Barclay, D.J., Calkin, P.E., Wiles, G.C., 2001. Holocene history of Hubbard Glacier in Yakutat Bay and Russell Fiord, southern Alaska. Geologic Society of America Bulletin, 113: 388–402.

Bednarŝek, N., Tarling, G.A., Bakker, D.C.E., Fielding, S., Jones, E.M., Venables, H. J., Ward, P., Lézé, B., Feely, R.A., Murphy, E.J., 2012. Extensive dissolution of live pteropods in the Southern Ocean. Nature Geosciences, 5: 881–885. doi:10.1038/ngeo1635

Bowen, G.J., Wilkinson, B., 2002. Spatial distribution of $\delta^{18}O$ in meteoric precipitation. Geology, 30(4): 315–318.

Brown, G.H., 2002. Glacier meltwater hydrochemistry. Applied Geochemistry, 17: 855–883.

Cai, W.J., Dai, M., Wang, Y., Zhai, W., Huang, T., Chen, S., Zhang, F., Chen, Z., Wang, Z., 2004. The biogeochemistry of inorganic carbon and nutrients in the Pearl River estuary and the adjacent Northern South China Sea. Continental Shelf Research, 24: 1301–1319.

Cai, W.J., Chen, L., Chen, B., Gao, Z., Lee, S.H., Chen, J., Pierrot, D., Sullivan, K., Wang, Y., Hu, X., Huang, W.J., Zhang, Y., Xu, S., Murata, A., Grebmeier, J.M., Jones, E.P., Zhang, H., 2010. Decrease in the CO_2 uptake capacity in an ice-free Arctic Ocean basin. Science, 329: 556–559.

Caldeira, K., Wickett, M.A., 2003. Anthropogenic carbon and ocean pH. Nature, 425: 365.

Cokelet, E.D., Jenkins, A.J., Etherington, L.L., 2007. A transect of Glacier Bay ocean currents measured by acoustic Doppler current profiler (ADCP), in Piatt, J.F., and Gende, S.M., eds., Proceedings of the Fourth Glacier Bay Science Symposium, October 26–28, 2004. U.S. Geological Survey Scientific Investigations Report 2007, 5047: 80–83.

Cross, J.N., Mathis, J.T., Bates, N.R., Byrne, R.H., 2013. Conservative and non-conservative variations of total alkalinity on the Southeastern Bering Sea Shelf. Marine Chemistry, 154: 100–112. doi:10.1016/j.marchem.2013.05.012

Dickson, A.G., Millero, F.J., 1987. A comparison of the equilibrium constants for the dissociation of carbonic acid in seawater media. Deep Sea Research, 34: 1733–1743. doi:10.1016/0198-0149(87)90021-5

Dickson, A.G., 1990. Standard potential of the reaction: $AgCl_{(s)}+ ½H_{2(g)}=Ag_{(s)}+HCl_{(aq)}$, and the standard acidity constant of the ion HSO_4^- in synthetic seawater from 273.15 to 318.15. The Journal of Chemical Thermodynamics, 22, 113–127. doi:10.1016/0021-9614(90)90074-Z

Etherington, L.L., Hooge, P.N., Hooge, E.R., Hill, D.F., 2007. Oceanography of Glacier Bay, Alaska: implications for biological patterns in a glacial fjord estuary. Estuaries and Coasts, 30(6): 927–944.

Evans, W., Mathis, J.T., Cross, J.N., 2014. Calcium carbonate corrosivity in an Alaskan inland sea. Biogeosciences, 11: 365–379. doi:10.5194/bg-11-365-2014

Feely, R.A., Sabine, C.L., Lee, K., Berelson, W., Kleypas, J., Fabry, V.J., Millero, F.J., 2004. Impact of anthropogenic CO_2 on the $CaCO_3$ system in the oceans. Science, 305: 362–366. doi:10.1126/science.1097329.

Feely, R.A., Alin, S.R., Newton, J., Sabine, C.L., Warner, M., Devol, A., Krembs, C., Maloy, C., 2010. The combined effects of ocean acidification, mixing, and respiration on pH and carbonate saturation in an urbanized estuary. Estuarine, Coastal and Shelf Science, 88: 442–449. doi:10.1016/j.ecss.2010.05.004

Goodwin, R.G., 1988. Holocene glaciolacustrine sedimentation in Muir Inlet and ice advance in Glacier Bay, Alaska, U.S.A. Arctic Alpine Research, 20: 55–69.

Hill, D.F., Ciavola, S.J., Etherington, L., Klaar, M.J., 2009. Estimation of freshwater runoff into Glacier Bay, Alaska and incorporation into a tidal circulation model. Estuarine, Coastal and Shelf Science, 82: 95–107.

Hooge, P.N., Hooge E.R., 2002. Fjord oceanographic processes in Glacier Bay, Alaska. Glacier Bay Report, 1–148.

Johnson, A.J., Larsen, C.F., Murphy, N., Arendt, A.A., Zirnheld, S.L., 2013. Mass balance in the Glacier Bay area of Alaska, USA, and British Columbia, Canada, 1995-2011, using airborne laser altimetry. Journal of Glaciology, 59: 632–648.

Larsen, C.F., Motyka, R.J., Freymueller, J.T., Echelmeyer, K.A., Ivins, E.R., 2005. Rapid viscoelastic uplift in southeast Alaska caused by post-Little Ice Age glacial retreat. Earth and Planetary Science Letters, 237: 548–560.

Lawson, D.E., 2004. An overview of selected glaciers in Glacier Bay. USGS Glacier Bay Report, 1-6.

Lewis, E., Wallace D.W.R., 1998. CO2SYS – program developed for CO_2 system calculations, Report ORNL/CDIAC-105 (Carbon Dioxide Information and Analysis Centre), Oak Ridge National Lab., U.S. Department of Energy.

Mathis, J.T., Cross, J.N., Bates, N.R., 2011a. Coupling primary production and terrestrial runoff to ocean acidification and carbonate mineral suppression in the Eastern Bering Sea. Journal of Geophysical Research, 116: 1–24. doi:10.1029/2010JC006453.

Mathis, J.T., Cross, J.N., Bates, N.R., 2011b. The role of ocean acidification in systemic carbonate mineral suppression in the Bering Sea. Geophysical Research Letters, 19(38): 1–6. doi: 10.1029/2011GL048884

Mathis, J.T., Questel, J.M., 2013. Assessing seasonal changes in carbonate parameters across small spatial gradients in the Northeastern Chukchi Sea. Continental Shelf Research, 67: 42–51. doi:10.1016/j.csr.2013.04.041

Matthews, J.B., 1981. The seasonal circulation of the Glacier Bay, Alaska fjord system. Estuarine, Coastal and Shelf Science, 12: 679–700.

Mehrbach, C., Culberson, C.H., Hawley, J.E., Pytkowicz, R.M., 1973. Measurement of the apparent dissociation constants of carbonic acid in seawater at atmospheric pressure. Limnology and Oceanography, 18: 897–907.

Miller, A.W., Reynolds, A.C., Sobrino, C., Riedel, G.F., 2009. Shellfish face uncertain future in high CO_2 world: influence of acidification on oyster larvae calcification and growth in estuaries. PloS one, 4: e5661.

Milner, A.M., Fastie, C.L., Chapin III, F.S., Engstrom, D.R., Sharman, L.C., 2007. Interactions and linkages among ecosystems during landscape evolution. Bioscience, 57: 237–247. doi:http://dx.doi.org/10.1641/B570307

Mucci, A., 1983. The solubility of calcite and aragonite in seawater at various salinities, temperatures, and one atmosphere total pressure. American Journal of Science, 283: 780–799.

Orr, J.C., Fabry, V.J., Aumont, O., Bopp, L., Doney, S.C., Feely, R. a, Gnanadesikan, A., Gruber, N., Ishida, A., Joos, F., Key, R.M., Lindsay, K., Maier-Reimer, E., Matear, R., Monfray, P., Mouchet, A., Najjar, R.G., Plattner, G.-K., Rodgers, K.B., Sabine, C.L., Sarmiento, J.L., Schlitzer, R., Slater, R.D., Totterdell, I.J., Weirig, M.-F., Yamanaka, Y., Yool, A., 2005. Anthropogenic ocean acidification over the twenty-first century and its impact on calcifying organisms. Nature, 437: 681–686.

Pfeffer, W.T., Cohn, J., Meier, M.F., Krimmel, R.M., 2000. Alaskan glacier beats a rapid retreat. Eos Transactions American Geophysical Union, 81(48): 577–584.

Renner, M., Arimitsu, M.L., Piatt, J.F., 2012. Structure of marine predator and prey communities along environmental gradients in a glaciated fjord. Canadian Journal of Fisheries and Aquatic Sciences, 69: 2029–2045.

Sabine, C.L., Feely, R.A., Gruber, N., Key, R.M., Lee, K., Bullister, J.L., Wanninkhof, R., Wong, C.S., Wallace, D.W.R., Tilbrook, B., Millero, F.J., Peng, T. H., Kozyr, A., Ono, T., Rios, A.F., 2004. The oceanic sink for anthropogenic CO_2. Science, 305: 367–371. doi:10.1126/science.1097403

Schlitzer, R., 2013. Ocean data view, http://odv.awi.de.

Sharman, L., 2010. Driving the marine ecosystem: oceanography as a key long-term monitoring vital sign at Glacier Bay National Park and Preserve. Alaska Park Science, 9: 36–39.

Uppström, L.R., 1974. The boron/chlorinity ratio of deep-sea water from the Pacific Ocean. Deep Sea Research, 21: 161–162. doi:10.1016/0011-7471(74)90074-6

Wanninkhof, R., Park, G.H., Takahashi, T., Sweeney, C., Feely, R., Nojiri, Y., Gruber, N., Doney, S.C., McKinley, G. A., Lenton, A., Le Quéré, C., Heinze, C., Schwinger, J., Graven, H., Khatiwala, S., 2013. Global ocean carbon uptake: magnitude, variability and trends. Biogeosciences, 10: 1983–2000.

Chapter 3:

Assessing Net Community Production in a Glaciated Alaska Fjord[1]

3.0 Abstract

The impact of deglaciation in Glacier Bay National Park and Preserve (GLBA), Alaska, has been observed to seasonally impact the biogeochemistry of this marine system. The influence from surrounding glaciers, particularly tidewater glaciers, has the potential to greatly impact the efficiency and structure of the marine food web within GLBA. To assess the magnitude, spatial and temporal variability of net community production (NCP) in a glaciated fjord, we measured dissolved inorganic carbon (DIC), inorganic macronutrients, dissolved oxygen (DO), and particulate organic carbon (POC) between July 2011 and July 2012 in GLBA. Seasonally averaged data were analyzed on a regional basis to account for distinct biogeochemical differences within the bay due to spatial variation in rates of primary production and the influence of glacial-fed stratification, particularly in the northern regions. High NCP rates were observed across the bay (~54 to ~81 mmoles C m^{-2} d^{-1}) between the summer and fall of 2011. However, between the fall and winter, as well as between the winter and spring of 2012, air-sea fluxes of CO_2 and organic matter respiration made NCP rates negative across most of the bay as inorganic carbon and macronutrient concentrations returned to pre-bloom levels. The highest carbon production occurred within the lower bay during the transition from summer to fall in 2011 with ~$1.3x10^{10}$ g C $season^{-1}$. Bay-wide, carbon production over the summer and fall was ~$2.6x10^{10}$ g C $season^{-1}$. Respiration and air-sea gas exchange were the dominant drivers of carbon biogeochemistry over the fall and winter of 2012. The substantial spatial and temporal variability in our NCP estimates largely reflect glacial influences within the bay, as melt-water is depleted in macronutrients relative to marine waters entering from the Gulf of Alaska in the middle and lower parts of the bay. Further glacial retreat will likely lead to additional modifications in the carbon biogeochemistry of GLBA, with unknown consequences for the local marine food web that leads up to many species of marine mammals.

[1] In Revision: Reisdorph, S.C., Mathis, J.T., 2014. Assessing net community production in a glaciated Alaska fjord. Biogeosciences.

3.1 Introduction

Glacier Bay (GLBA) lies within the Gulf of Alaska's (GOA) coastal ocean and is a pristine glacially influenced fjord that is representative of many other estuarine systems that border the GOA (Figure 3.1). GLBA is influenced by freshwater input, primarily from many surrounding alpine and tidewater glaciers. The low-nutrient influx of freshwater into GLBA, which is highest (up to ~40% freshwater in surface waters during the summer; Reisdorph and Mathis, 2014) along the northern regions of the bay, affects the nutrient loading and, thus, biological production and CO_2 fluxes within the bay. The southern region of the bay is less affected by this runoff due to distance from the glacial influence and is more influenced by marine waters that exchange through a narrow channel with a shallow entrance sill.

Alaska's coasts contain more than 200 major fjords, though very few have been studied in detail (Etherington et al., 2007). They can be grouped into two distinct regions, a south-central region and a southeast region, each with hydrological differences due to differences in terrestrial and oceanic influences. The south-central fjords, which include those within Cook Inlet and Prince William Sound (PWS) (Figure 3.1), tend to have more open interaction with the oceanic waters of the GOA, while fjords in the southeast, such as GLBA, communicate with the GOA via smaller interconnected channels (Etherington et al., 2007). Glacial influences play an important role in both of these fjord systems, but are more dominant in locations such as GLBA where estuarine-ocean exchange is limited. While PWS and GLBA are highly glacially influenced and have similar source waters derived from the coastal GOA, PWS is a semi-enclosed fjord that has a relatively direct exchange of waters via Hinchinbrook Entrance and Montague Strait (Musgrave et al., 2013). Conversely, GLBA has only one entrance over a shallow entrance sill (~25 m) (Hooge and Hooge, 2002) and connects to the GOA through several small channels (Hill et. al., 2009).

Despite GLBA's limited exchange with the open ocean, elevated chlorophyll-*a* (chl. *a*) concentrations have been observed throughout most of the year, especially from spring through fall (Etherington et. al., 2007), and primary production supports a diverse food web that lead up to endangered species such as humpback whales and Stellar sea lions. Over the past ~250 years, GLBA has experienced very rapid deglaciation, which has likely impacted the biological structure of the bay. As the climate continues to warm, additional changes to this ecosystem and

marine populations have the potential to impact net community production (NCP) within the bay, with cascading effects through the food web, as has been noted in the GOA in regards to decreasing capelin populations (Arimitsu et al., 2008). To better understand the seasonal dynamics of the underlying biogeochemistry in GLBA, we used the seasonal drawdown of the inorganic constituents of photosynthesis within the mixed layer to estimate regional mass flux of carbon and rates of NCP along with air-sea flux rates of CO_2. This approach has been used in other high-latitude regions to assess ecosystem functionality (e.g. Mathis et al., 2009; Cross et al., 2012; Mathis and Questel, 2013).

Previous studies have shown there is wide-ranging variability in rates of primary production within glaciated fjord systems, though NCP data within these ecosystems are sparse. However, larger scale studies have estimated production within the Pacific Ocean. A study by Whitney (2011) looked at nutrient availability and new production in the subarctic Pacific Ocean between 1987 and 2010. He estimated new production between April and September of ~7.4 mmoles C m^{-2} d^{-1} off of the Canadian coast (48°-54°N, 140°-128°W) and ~5.5 mmoles C m^{-2} d^{-1} along the subarctic-subtropical boundary in the north-central Pacific Ocean (36°-41°N, 170°-150°W). A comprehensive analysis done by Lockwood et al. (2012) combined previous NCP estimates within the Pacific and GOA regions using a ratio of dissolved oxygen to argon for their NCP calculations. Averaging NCP calculations from their study, as well as multiple published data, they estimated daily NCP around Ocean Station Papa (~50°N - 55°N, 145°W) of 14 ± 5 mmoles C m^{-2} d^{-1}. Additional NCP estimates were done for the northern Pacific region near a chlorophyll front (40°N-45°N) where rates were 9 ± 5 mmoles C m^{-2} d^{-1} and within the Alaska Gyre (~50°N-55°N) where rates were 18 mmoles C m^{-2} d^{-1} (Lockwood et al., 2012).

The few NCP studies done in fjord systems similar to that of GLBA have used a variety of instruments and data in their NCP estimations. Using chl. *a* data collected via a FIRe (Satlantic Instruments) fluorometer, Quigg et al. (2013) found integrated primary productivity within Simpson and Sheep Bays, PWS, varied from ~ 60 to ~90 mmoles C m^{-2} d^{-1}. These values are between those estimated by Ziemann et al. (1991) in Auke Bay, AK during summer seasons between 1985 and 1989 (~8 mmoles C m^{-2} d^{-1}) and those from Goering et al. (1973) in and near Port Valdez, AK using ^{14}C (~125 to ~333 mmoles C m^{-2} d^{-1}).

A study by Aracena et al. (2011) looked at water column productivity in response to surface sediment export production in various Chilean Patagonian fjords (41-56°S). They

divided the fjords into four latitudinal regions and calculated primary production rates during the summer between ~35 mmoles C $m^{-2} d^{-1}$ in the more southern regions (52°S - 55°S) and ~488 C $m^{-2} d^{-1}$ to the north (41°S - ~44°S). Fjords within the Central Patagonia region (48°S – 51°S) are strongly influenced by glaciated terrain and freshwater runoff, similar to influences in and around GLBA. In Central Patagonia, Aracena et al. (2011) estimated primary productivity at ~57 mmoles C $m^{-2} d^{-1}$ in the spring and found primary production rates comparable to those of Norwegian fjords (~9 to ~360 mmoles C $m^{-2} d^{-1}$).

Few regions of the world still have tidewater glaciers, and Alaskan fjords, such as GLBA, is one such region, along with Greenland, Svalbard, Antarctica, Chile, and the Canadian Arctic (Syvitski et al., 1987; Etherington et al., 2007). Therefore, understanding the dynamics that drive NCP and the associated air-sea CO_2 fluxes within glacially influenced Alaskan fjords can provide insights on how deglaciation may affect carbon budgets in fjords worldwide.

3.2 Background

Seasonal variation in factors such as light availability and freshwater input impact physical conditions that are vital to primary production including stratification, photic depth, and nutrient availability. These drivers of NCP vary temporally and spatially within GLBA. Increasing solar radiation during spring and summer help to set up the stratification needed for photosynthetic organisms to remain in the mixed layer and longer daylight hours promote photosynthesis. Low-nutrient glacial runoff is prevalent, and while it aids in stratification, its low macronutrient concentrations dilute available nutrients in the northern regions nearest tidewater outflows. In the lower parts of the bay, glacial influence is lower and macronutrients are more abundant allowing higher levels of primary production during spring and summer.

GLBA maintains relatively elevated phytoplankton concentrations throughout the year compared to levels observed in similar Alaskan fjords (Hooge and Hooge, 2002). However, insufficient research has been done on the biological system within GLBA to understand why this occurs. One of the more comprehensive studies (Robards et al., 2003) found zooplankton diversity and abundance to be similar to that throughout the GOA. Within GLBA, areas nearest tidewater glaciers, or recently grounded tidewater inlets, maintained some of the highest prey species (i.e., zooplankton and forage fish) abundances, suggesting the ecological importance of these tidewater–influenced habitats. Forage fish, including capelin, sand lance and walleye

Pollock, along with euphausids, were generally found the upper inlets and areas near river and stream outlets. Robards et al. (2003) also found differing fish community structures in the east and west arms of the bay, with the east arm primarily supporting capelin with Pollock dominating elsewhere in the bay. In regards to top predators (sea birds and marine mammals) in GLBA, Robard et al. (2003) found assemblages to be seasonally dependent, but numerous and diverse. Similar to observations in the GOA and Auke Bay, AK, a peak in zooplankton abundance occurs during late May or early April within lower GLBA. However, unlike the GOA and other estuaries along the GOA, a second, smaller peak in zooplankton abundance occurred in August, though zooplankton densities within the upper regions of the bay generally peak in July (Robard et al., 2003).

During the summer, GLBA is also a crucial locale for several marine predators, some of whose populations are declining due to climate change and deglaciation. Spawning and non-spawning adult capelin, a prey species for several marine predators, are more likely to occur in areas nearest tidewater glaciers that have lower temperatures and chl. *a* levels coupled with higher turbidity and dissolved oxygen concentrations as compared to other areas of GLBA (Arimitsu et al., 2008). In the GOA, populations of capelin, as well as other favored prey species, have been observed to be declining in association with a reduction of these glacially-influenced habitats and have been linked to reduced populations of higher trophic level predators including harbor seals and red-legged kittiwakes (Piatt and Anderson, 1996; Trites and Donnelly, 2003; Arimitsu et al, 2008;). GLBA sustains perhaps one quarter of the worldwide population of breeding Kittlitz's Murrelets (Arimitsu et al., 2008), a seabird classified as critically endangered and proposed for listing under the U.S. Endangered Species Act by the International Union for the Conservation of Nature (IUCN) (Kirchhoff et al., 2014).

Macronutrient concentrations also vary spatially across the bay, partially due to dilution from the low-nutrient glacial influence in the north. These nutrient concentrations are also affected by the metabolic requirements of phytoplankton taken up at average proportions for carbon, nitrogen and phosphate of 106:16:1 (e.g., Weber and Deutsch, 2010), referred to as the Redfield ratio. Macronutrient uptake within the southern regions of the GLBA closely follows the Redfield ratio (Reisdorph and Mathis, 2014). However, the northern regions are highly influenced by low-macronutrient glacial runoff, resulting in nutrient uptake that deviates from the Redfield ratios and reduced nutrient concentrations in the surface water within these glacial

outflow regions (Reisdorph and Mathis, 2014).

Reisdorph and Mathis (2014) found dissolved inorganic carbon (DIC) and total alkalinity (TA) concentrations to be lowest within the upper arms of GLBA, while concentrations increased to the south throughout the year, with the largest gradient occurring during summer. However, they found waters across the bay to be well-mixed throughout the water column during winter due to a higher degree of seasonal wind mixing. A similar pattern was observed in the aragonite saturation states (Ω_A) within the bay, with aragonite undersaturation occurring within the upper arms of the bay during though summer. During the fall, Ω_A were tightly constrained and all surface waters were undersaturated with respect to aragonite.

Aside from primary production, air-sea carbon dioxide (CO_2) flux also impacts carbon concentrations within surface waters. Evans and Mathis (2013) observed instances of both, atmospheric uptake and outgassing, to occur in almost every month in the coastal regions of the GOA, which are the source waters of GLBA. However, uptake of atmospheric CO_2 dominated during the non-winter months, especially in the spring and fall, which coincided with periods of strong winds and undersaturated pCO_2 levels in the surface waters. When annually-averaged, they report that the coastal ocean and continental margin of the GOA act as a strong sink for atmospheric CO_2 with fluxes of -2.5 and -4.0 mmoles CO_2 m^{-2} d^{-1}, but their observations were limited in glacially-influenced waters.

For this paper, we have calculated seasonal NCP and air-sea carbon flux for four regions within GLBA in order to better understand primary production in a glacially dominated environment, representative of much of the southern coastal AK region.

3.3 Methods

Ten oceanographic sampling cruises took place between July 2011 and July 2012. Water column samples were collected at six depths (2, 10, 30, 50,100 m and near the bottom) at each station throughout the bay (Figure 3.1). Seasonal data were calculated by averaging each measured parameter at each depth for all cruises during the respective seasons. The summer season consisted of June, July and August, fall included September and October; winter was comprised of February and March cruises, and the spring season included the months of April and May. Data were averaged regionally within each of four regions of the bay (lower bay = LB; central bay = CB; east arm = EA; west arm = WA) (Figure 3.1).

Conductivity-temperature-depth (CTD) data were collected on downcasts with a Seabird 19-plus system. Dissolved oxygen (DO) was sampled and processed first to avoid compromising the samples by atmospheric gas exchange. Samples for DO analysis were drawn into individual 115 ml Biological Oxygen Demand (BOD) flasks that were rinsed with 4-5 volumes of sample, filled with sample, treated with 1 mL $MnCl_2$ and 1 mL NaI/NaOH, plugged, and the neck filled with DI water to avoid atmospheric exchange. Samples were analyzed using Winkler titrations within 48 hours. Apparent oxygen utilization (AOU) was derived from observed DO concentrations using Ocean Data View calculations in version 4.6.2 (Schlitzer, 2013).

DIC samples were drawn into 250 mL borosilicate bottles. Samples were fixed with a saturated mercuric chloride solution (200 µl), the bottles sealed, and stored until analysis at the Ocean Acidification Research Center (OARC) at the University of Alaska Fairbanks (UAF). High-quality DIC data were attained by using a highly precise (0.02%; 0.4 µmoles kg^{-1}) VINDTA 3C-coulometer system. TA was determined by potentiometric titration with a precision of ~1 µmoles kg^{-1}. DIC and TA samples were calibrated by routine analysis of seawater certified reference materials (prepared and distributed by Andrew Dickson, UCSD) to ensure accuracy.

Macronutrient samples were filtered through 0.8 µm Nuclepore filters using in-line polycarbonate filter holders into 25 ml HDPE bottles and frozen (-20°C) until analysis at UAF. Samples were analyzed within several weeks of collection using an Alpkem Rapid Flow Analyzer 300 and following the protocols of Whitledge et al. (1981).

Particulate organic carbon (POC) samples were collected from Niskins into brown 1 L Nalgene bottles and stored for filtering within 2 days of collection. A known volume of well-mixed sample was filtered through muffled and preweighed 13 mm glass fiber filters using a vacuum pump. Filtered sampled were frozen for transport back to UAF where they were then dried and reweighed. Analyses were completed by OARC at UAF and were run using the methods outlined in Goñi et al. (2003).

The partial pressure of CO_2 (pCO_2) was calculated using CO2SYS (version 2.0), a program that employs thermodynamic models of Lewis and Wallace (1998) to calculate marine carbonate system parameters. A standard atmospheric pCO_2 of 395 µatm was used for all seasons. For this study, we used K_1 and K_2 constants from Mehrbach et al., (1973) and refitted by Dickson and Millero (1987), $KHSO_2$ values from Dickson (1990), the seawater pH scale, and $[B]_T$ value from Uppström (1974).

CO_2 fluxes were calculated using seasonally averaged seawater temperature, wind speed, and seawater and atmospheric pCO_2 data using the equation,

$$\text{Flux} = L * (\Delta pCO_2) * k \quad \text{(Eq. 3.1)}$$

where L is the solubility of CO_2 at a specified seawater temperature in mmoles m^{-3} atm^{-1} and ΔpCO_2 represents the difference between seawater and atmospheric pCO_2 in µatm. k is the steady/short-term wind parameterization in cm hr^{-1} at a specified wind speed and follows the equation,

$$k = 0.0283 * U *(Sc/660)^{(-½)} \quad \text{(Eq. 3.2)}$$

where U is wind speed in m s^{-1}, *Sc* is Schmidt number, or the kinematic velocity of the water divided by the molecular diffusivity of a gas in water and normalized to 660 cm hr^{-1}, equivalent to the *Sc* for CO_2 in 20°C seawater (Wanninkhof and McGillis, 1999).

Seawater temperatures for flux calculations were taken from surface bottle CTD data. Wind speeds were obtained from a Bartlett Cove, AK weather station (Station BLTA2) located in GLBA and maintained by the National Weather Service Alaska Region.

NCP calculations were made using the seasonal drawdown of DIC within the mixed layer (upper 30 m) and were normalized to a salinity of 35 to account for the high glacial influence in the northern regions of GLBA. NCP production was calculated for each season between the summer of 2011 and the summer of 2012 according to the equation (Williams, 1993),

$$\text{NCP} = DIC_{season2} - DIC_{season1} \quad \text{(Eq. 3.3)}$$
$$= \Delta DIC \text{ (moles C per unit volume area)}$$

Since Eq. 3.3 only reflects the effects of DIC, and not alkalinity, this could be accounted for by correction of the seasonal changes in TA (Lee, 2001) using the equation,

$$\Delta DIC_{Alk} = 0.5*(\Delta Alk + \Delta NO_3) \quad \text{(Eq. 3.4)}$$

and subtracting this value from the seasonal change in salinity-normalized DIC (nDIC).Including this correction factor in NCP calculations, it provides an NCP estimate in which biological production is the significant process influencing the seasonal changes to DIC concentrations (Bates et al., 2005; Mathis et al., 2009; Cross et al., 2012). Air-sea gas exchange can play a lesser role in NCP variation and these are discussed in Section 3.4.5.

Figures 3.1 through 3.6 were created using Ocean Data View (ODV) version 4.6.2 (Schlitzer, 2013). Figure 3.7 was created in Microsoft Excel 2008 version 12.3.6.

3.4 Results and Discussion

3.4.1 Spatial and seasonal distributions of DIC and nitrate

DIC and nitrate are important inorganic components that are consumed during photosynthesis at various rates throughout the year in GLBA. Figure 3.2 shows the seasonal relationship between DIC, nitrate and depth between the summer of 2011 and the summer of 2012, with the red line depicting the C:N Redfield Ratio of 106:16.

DIC concentrations during the summer of 2011 ranged from ~1400 to 2100 μmoles kg^{-1}. DIC variability in the surface waters was a result of primary production and dilution from glacial discharge (Reisdorph and Mathis, 2014), and had a large range (~1400 to 2000 μmoles kg^{-1}) with the lowest concentrations in the two arms of GLBA due to the greater influence of tidewater glacier runoff, as well as the upper-CB, where, seasonally, chl *a* concentrations have been observed to be highest (Etherington et al., 2007). Below the surface layer, DIC and nitrate concentrations closely followed the Redfield ratio and were fairly constant throughout the year.

Nitrate concentrations throughout the water column during the summer of 2011 ranged from ~2.5 to ~37.0 μmoles kg^{-1}, with slightly less variability in the surface layer (~2.5 and 24.0 μmoles kg^{-1}). Surface nitrate concentrations were low, but remained >5.0 μmoles kg^{-1} at all stations, even during times of elevated primary production. Nitrate values were consistently the lowest in the two arms and CB. While there was a large drawdown of nitrate, particularly in spring and summer (as much as 20.0 μmoles kg^{-1} when compared to winter concentrations), surface waters were not depleted at any of the observed stations, indicating that nitrate was being continuously supplied to the surface layer. Additionally, phosphate concentrations (data not shown here) remained above ~0.5 μmoles kg^{-1}, indicating that it was not the limiting reagent to photosynthesis either. The lowest concentrations of DIC and macronutrients were observed within the two arms due to the influence tidewaters glacier runoff, which can likely be attributed to dilution from freshwater runoff, as well as salinity-driven stratification limiting mixing and nutrient replenishment in the mixed layer. Additionally, the unique chemistry of tidewater glacier discharge relative to alpine and stream discharge likely played an important role. Because several glaciers in GLBA are calving directly into the water rather than travel down streambeds that are rich in carbonate and organic sediments, there is little opportunity for the glacial melt to accumulate macronutrients, as is the case with carbonate alkalinity (Reisdorph and Mathis, 2014).

In the fall of 2011, DIC and nitrate concentrations increased in the surface waters as primary production slowed and wind mixing increased. DIC concentrations in surface waters ranged from ~1700 μmoles kg^{-1} to 2040 μmoles kg^{-1}, while below the surface, DIC concentrations reached ~2075 μmoles kg^{-1}. Nitrate concentrations during this time were between ~12 μmoles kg^{-1} and 32 μmoles kg^{-1}. Due to decreasing primary production, concentrations were similar within surface waters, ranging from 11 μmoles kg^{-1} to 30 μmoles kg^{-1}, with the lowest concentrations observed in the arms.

Increased wind mixing and the reduction of glacial input during the winter of 2012 led to full water column mixing, with much more constrained DIC concentrations (~1920 μmoles kg^{-1} to 2075 μmoles kg^{-1}) than during previous seasons and no significant difference between surface concentrations and those at depth. Nitrate concentrations were also similar to those of fall, ranging from ~12 μmoles kg^{-1} to 33 μmoles kg^{-1}. During winter, DIC and nitrate concentrations fell near the Redfield ratio but deviated slightly from Redfield at the highest nitrate concentrations (Figure 3.2). This may have been due to nitrification of ammonium by bacteria, leading to an increase in the nitrate concentration. Another possibility is 'carbon overconsumption', the process in which more DIC is taken up than that inferred from the C:N Redfield ratio (Voss et al., 2011). Explanations for carbon overconsumption include the preferential remineralization of organic nitrogen (Thomas and Schneider, 1999) or an increased release of dissolved organic carbon (DOC) (Engel et al., 2002; Schartau et al., 2007).

As temperatures began to warm in the spring of 2012, the onset of glacial melt and primary production reduced DIC and nitrate concentrations in surface waters across the bay. Surface DIC concentrations were between ~1750 μmoles kg^{-1} and 2025 μmoles kg^{-1}, with water column concentrations reaching ~2075 μmoles kg^{-1} (Figure 3.2). Water column nitrate concentrations ranged from ~7 μmoles kg^{-1} to ~ 31 μmoles kg^{-1}, with an observed surface water maximum of ~20 μmoles kg^{-1}. During the spring, DIC and nitrate correlated closely with the Redfield ratio except for two surface samples located at the northernmost ends of each arm (Figure 3.2). This deviation may be explained by the fact that these stations were the first to be influenced by glacial runoff during the onset of the glacial melt season.

Further drawdown of DIC and nitrate in surface waters was observed during the summer of 2012 as primary production intensified. Low nutrient glacial runoff was also highest at this time of year, affecting surface water macronutrient concentrations within the arms of the bay

(Hooge and Hooge, 2002). However, concentrations did not drop as low as was observed during the previous summer. In 2012, DIC concentrations were between ~1545 to 2066 μmoles kg^{-1}, while the surface waters had a maximum of ~2000 μmoles kg^{-1}. Similar to the previous summer, macronutrients did not reach depletion during the summer of 2012, implying they were not limiting primary productivity, possibly due to nutrient replenishment via tidal pumping. Nitrate concentrations varied from ~13 to 33 μmoles kg^{-1}, with relatively high surface concentrations between ~17 and 31 μmoles kg^{-1}. As shown in Figure 3.2, the surface nitrate concentration continued to deviate from the Redfield ratio as these macronutrients were increasingly drawn down by primary productivity and diluted by tidewater glacier runoff. The stations most affected were those within the east and west arms, as well as upper CB, where freshwater influence was greatest. Within the LB, mixing of nutrient-rich marine waters from the GOA likely offset much of the drawdown from primary production and allowed these surface waters to fall closer to the Redfield ratio.

3.4.2 Rates and Masses of NCP

As mentioned above (Section 3.3), DIC concentrations in the upper 30 m of the water column, representing the mixed layer depth (MLD), were averaged and normalized to a salinity of 35 in order to estimate rates and masses of NCP between seasons (Figure 3.3). The seasonal transition between the summer and fall of 2011 had the largest rates of NCP observed during the year of study. During this time all NCP rates were positive, signifying enhanced primary productivity in the mixed layer. NCP rates were highest within the east and west arms of the bay at 70.3 ± 3.5 and 81.3 ± 4.1 mmoles C m^{-2} d^{-1}, respectively. A similar NCP rate of 68.9 ± 3.4 mmoles C m^{-2} d^{-1} was observed in LB, while CB had the lowest rate of 53.6 ± 2.7 mmoles C m^{-2} d^{-1}. Calculated rates of NCP became negative during the seasonal transitions from fall to winter, as well as from winter to spring. These negative NCP values indicate that air-sea fluxes (discussed in Section 3.4.5) and organic matter respiration were prominent, increasing CO_2 (DIC) concentrations in the surface waters and overwhelming any weaker signal from primary production.

Air-sea flux of CO_2 overwhelmed the biological signal in all regions of GLBA between the fall and winter seasons. Between the fall and winter, the LB experienced the highest degree of CO_2 flux when compared to biological production with a calculated NCP rate of -14.2 ± 0.7

mmoles C m^{-2} d^{-1}, followed closely by the CB at -11.5 ± 0.6 mmoles C m^{-2} d^{-1}. The biological production was overwhelmed by CO_2 influx in the east and west arms (-0.5 ± 0.03 and -1.3 ± 0.1 mmoles C m^{-2} d^{-1}), respectively, but to a lesser degree than in regions to the south.

A similar trend was observed between the winter and spring of 2012 in all regions except for the LB, likely due to its more macronutrient-rich marine influence from the GOA. The CO_2 flux signal exceeded NCP within the east and west arms of the bay, with rates of -36.4 ± 1.8 mmoles C m^{-2} d^{-1} and -26.6 ± 1.3 mmoles C m^{-2} d^{-1}, respectively, and to a lesser degree in CB with -17.5 ± 0.9 mmoles C m^{-2} d^{-1}. The LB was the only region where biological production dominated the CO_2 flux with a positive NCP rate of 17.6 ± 0.9 mmoles C m^{-2} d^{-1}, again reflecting the region's nutrient-rich marine influence.

Between the spring and summer of 2012 the primary production signal was evident in the NCP rates. The LB had the highest rate of NCP at 19.4 ± 1.0 mmoles C m^{-2} d^{-1}. CB and the EA had similar rates of 17.2 ± 0.9 and 15.7 ± 0.8 mmoles C m^{-2} d^{-1}, respectively. The WA displayed a lower rate of NCP at 6.0 ± 0.3 mmoles C m^{-2} d^{-1}, possibly the result of the strong low-macronutrient glacial influences along the arm, which may work to hinder production. Additionally, large volumes of glacial flour imparted into the surface waters from runoff during summer may have limited the photic depth and thus impeded some productivity in the upper arms of the bay (Etherington et al., 2007).

The total mass (g C $season^{-1}$) of carbon produced from NCP was also estimated for each season and are shown in Figure 3.4. The largest production of organic carbon occurred between the summer and fall of 2011, with the largest production signal in the LB and decreasing to the north as glacial influence increased. The LB had the largest biomass production of $1.3x10^{10}$ ± $6.5x10^{8}$ g C $season^{-1}$. The CB also had a large amount of production of $5.9x10^{9}$ ± $3.0x10^{8}$ g C $season^{-1}$, followed by the west and east arms with $4.9x10^{9}$ ± $2.5x10^{8}$ and $2.0x10^{9}$ ± $1.0x10^{9}$ g C $season^{-1}$, respectively. When summed across the bay, we found ~$2.6 x10^{10}$ ± $1.3x10^{9}$ g C $season^{-1}$ produced between the summer and fall of 2011.

As with the rates of NCP during seasonal transitions with low biological activity, the strong influence of air-sea CO_2 flux can be seen in the masses of carbon calculated. Any negative carbon masses indicate a gain in carbon within the surface waters as a result of low biological production and high wind-induced CO_2 flux and community respiration. Transitioning from fall to winter, there was substantial variability between the marine-dominated LB and the glacially-

influenced EA with $-1.7x10^{10} \pm 8.5x10^{8}$ g C season^{-1} and $-9.5x10^{7} \pm 4.8x10^{6}$ g C season^{-1}, respectively. Both regions were dominated by air-sea CO_2 flux. This difference between the northern and southern regions was likely the result of a higher degree of wind and tidal mixing at stations outside of and near the mouth of the bay. Carbon masses calculated from NCP in CB and the WA also indicated lower production and higher air-sea flux, having rates of $-5.0x10^{8} \pm 2.5x10^{7}$ g C season^{-1} and $-8.6x10^{9} \pm 4.3x10^{8}$ g C season^{-1}, respectively. Community respiration and air-sea flux led to a bay-wide total of ~ $-2.6x10^{10} \pm 1.3x10^{9}$ g C season^{-1}.

The production signal within the arms and central region of the bay continued to be overwhelmed by air-sea flux between the winter and spring of 2012. In the east and west arms masses were estimated at $-2.2x10^{9} \pm 1.1x10^{8}$ and $-3.3x10^{9} \pm 1.7x10^{8}$ g C season^{-1}, respectively, while the CB had a calculated value of $-4.1x10^{9} \pm 2.1x10^{8}$ g C season^{-1}. The LB once again had a positive NCP mass of $6.3x10^{9} \pm 3.2x10^{8}$ g C season^{-1}, signifying increased primary production and a decrease in air-sea flux in this region. Across the bay, we estimated a total of ~ $-3.3\ x10^{9} \pm 1.7x10^{8}$ g C season^{-1} between the winter and spring of 2012.

Between the spring and summer there was increased production across the bay as stratification strengthened and the hours of daylight increased. LB once again had the greatest production with $8.0x10^{9} \pm 4.0x10^{8}$ g C season^{-1}, followed by production within the CB of $4.5x10^{9} \pm 2.3x10^{8}$ g C season^{-1}. During this time of the year the east and west arms exhibited the lowest biomass production, with an NCP in the WA of $8.5x10^{8} \pm 4.3x10^{7}$ g C season^{-1} and $9.2x10^{7} \pm 4.6x10^{6}$ g C season^{-1} in the EA. NCP was likely hindered within the arms by the inundation of low-nutrient glacial runoff that formed a fresh surface layer and imparted glacial flour into the surface waters in these regions. NCP across the entire bay totaled ~$1.3x10^{10} \pm 6.5x10^{8}$ g C season^{-1}.

3.4.3 Spatial and seasonal distribution of POC

Particulate organic carbon (POC) concentrations were measured at three depths (surface, 50 m, and bottom) for each station and then averaged regionally. Figure 3.5 shows the regionally averaged POC concentrations and the color bar represents the apparent oxygen utilization (AOU) for each POC samples. During the summer of 2011 surface water POC concentrations were between ~12 and ~55 μmoles kg^{-1}. Station 20 at the head of the EA had the highest POC concentration at all sampled depths (~2m, ~50 m and ~160 m). POC concentrations in the

surface were ~46 μmoles kg^{-1} and ~ 42 μmoles kg^{-1} at depth, with a local minimum of ~30 μmoles kg^{-1} at 50 m. The elevated concentrations at this station may have been due to high erosion and sedimentation of the recently-grounded Muir glacier. When regionally averaged, the east and west arms had the highest surface POC concentrations of ~35 and ~33 μmoles kg^{-1}, respectively. The WA also exhibited high POC concentrations below the surface with ~33 μmoles kg^{-1} at 50 m and at depth. The arms also exhibited negative AOU of ~ -80 and ~ -64 μmoles kg^{-1} in the west and east arms, respectively. The highest positive AOU of ~105 μmoles kg^{-1} was observed in the bottom waters of the CB. Below the surface stations in the CB had similar POC concentration, at ~9 μmoles kg^{-1}, while the surface waters had a POC concentration of ~28 μmoles kg^{-1}, indicating relatively high primary production in the surface waters but little export to depth, perhaps due to reutilization within the surface waters or horizontal advection from tidal action. LB had relatively lower POC concentrations, but concentrations were similar at all depth with ~15 μmoles kg^{-1}. This could have been the result of higher turbulent mixing within the surface waters outside of the bay, leading to weaker stratification and increased vertical mixing as well as resuspension of POC sediment above and around the shallow entrance sill.

POC concentrations decreased rather dramatically, especially within the surface waters, as primary production slowed during the fall. A maximum regional POC concentration of ~13 μmoles kg^{-1} was observed in the surface waters of the WA while surface POC across the other regions were similar, falling between ~8 and ~9 μmoles kg^{-1}. Below the surface layer POC concentrations were low, ranging from ~5 to ~8 μmoles kg^{-1} at both 50 m and at depth. Regionally, all AOU values were positive during the fall of 2011, indicating widespread organic matter respiration. The maximum regional surface AOU (~82 μmoles kg^{-1}) was estimated for the LB and the minimum (~2 μmoles kg^{-1}) for the surface waters of the CB. During the fall the waters in the LB, especially across and seaward of the sill, were well mixed (Reisdorph and Mathis, 2014) and experienced a high degree of air-sea gas exchange (see section 3.4.5), which likely lowered the oxygen concentration. In this region, DIC concentrations were highest (~2050 μmoles kg^{-1} at all depths) and oxygen saturation was the lowest (not shown) of any region during fall, suggesting turbulent mixing enhanced air-sea flux, taking up DIC and outgassing oxygen.

In the winter of 2012, surface water POC concentrations did not exceed 20 μmoles kg^{-1} and AOU across the bay was on the order of ~70 μmoles kg^{-1}, suggesting little production was

occurring within the bay but respiration was still present. This is further supported by the negative NCP values described in Section 3.4.2. Surface POC concentrations during the winter ranged from ~2 to ~15 μmoles kg^{-1}, while POC concentrations at depth were similar, varying between ~3 and 16 μmoles kg^{-1}. When averaged regionally, the POC maximum in the WA of ~11 μmoles kg^{-1} was observed within the surface waters, while the CB had a subsurface maximum at 50 m of ~5 μmoles kg^{-1}. The EA and LB both had maximum POC concentrations in the bottom waters of ~14 and ~9 μmoles kg^{-1}, respectively. In the LB, where NCP was lowest, the bottom water POC concentration may have been the result of turbulent mixing outside of and across the sill of the bay, which can mix the water column to depth in this region (Reisdorph and Mathis, 2014; Etherington et al., 2007) and likely stir up sediments along the bottom. POC minima throughout the bay occurred at 50 m depth and ranged between ~2 and ~9 μmoles kg^{-1}, except at stations 24 in LB and station 13 within the CB where POC was at a local maximum at this depth.

POC concentration in the surface waters began to increase during the spring of 2012, primarily within northern regions of the bay. The EA had the greatest increase in surface POC (~62 μmoles kg^{-1}) with concentrations decreasing in the surface water towards the south. The WA and CB had similar surface POC concentrations of ~35 μmoles kg^{-1} and ~30 μmoles kg^{-1}, respectively. The LB had the lowest surface POC concentrations with ~13 μmoles kg^{-1}, while having the highest rate of NCP and AOU (~93 μmoles kg^{-1}). However, the LB subsurface and deep water POC concentrations were the highest of the four regions, ~9 μmoles kg^{-1} each, and the only region to have a positive AOU in bottom waters, suggesting a larger vertical transport of organic particles out of the surface layer than observed in other regions.

During the summer of 2012, all four regions exhibited regionally averaged POC maxima at the surface. Surface waters across the bay also experienced decreased AOU values and had elevated rates of NCP indicating substantial productivity within these waters. The EA had the highest surface concentration of POC with ~50 μmoles kg^{-1}, possibly the result of high productivity and strong stratification due to the buoyant glacial melt layer prohibiting particles from sinking out of the surface layer. Below the surface layer, POC concentrations decreased, ranging from ~4.5 to ~7.0 μmoles kg^{-1} at 50 m and ~5.0 to ~8.0 μmoles kg^{-1} at depth. The WA and CB regions had similar surface POC concentrations of ~23 μmoles kg^{-1}. Surface water across the bay also experienced the lowest AOU values and had high rates of NCP during summer,

signifying substantial productivity within these waters. The LB exhibited the lowest surface POC concentration with ~13 μmoles kg^{-1}, while experiencing the highest rate of NCP and AOU concentrations. This was likely the result of more rapid sinking rates of particles out of the surface waters as these waters were more turbulent than the glacially-stratified northern regions of the bay.

3.4.4 Relationship between DIC and DO

DIC and DO are both indicators of biological production in a marine ecosystem and have a C:O Redfield ratio of 106:-170 (Anderson and Sarmiento, 1994). Figure 3.7 shows the relationship of DIC and DO within Glacier Bay with the Redfield ratio shown by the red line. DIC and DO have an inverse relationship in that DIC is taken up during photosynthesis, while DO is produced, so we would expect high oxygen saturation states in spring and summer months.

During the summer of 2011, DO concentrations ranged from ~190 to ~400 μmoles kg^{-1}. All samples below the surface layer, as well as surface samples within the LB, followed the Redfield ratio, with concentrations at depth between ~190 and 280 μmoles kg^{-1}. Surface samples of stations within the arms and CB deviated from Redfield, having high DO concentrations and low DIC. Surface DO was higher than that at depth, ranging between ~230 and 400 μmoles kg^{-1}. The high DO concentrations, coupled with the reduced DIC concentrations in the surface waters, indicate enhanced levels of primary production during the summer season. However, in LB, DIC concentrations remained elevated (~2030 μmoles kg^{-1}) and DO concentrations were low (~240 μmoles kg^{-1}).

During fall DO concentrations decreased in the surface waters as temperatures cooled and wind mixing reduced stratification, hindering primary production within the surface waters. However, the surface samples within the arms and CB continued to deviate from Redfield. Surface DO concentrations ranged from ~210 to ~330 μmoles kg^{-1} coupled with reduced surface DIC concentrations, suggesting primary production was still occurring albeit at a lesser level than summer. At depth, DO concentrations varied between ~200 and 280 μmoles kg^{-1} with C:O ratios close to Redfield.

The water column throughout the bay was relatively well mixed during the winter of 2012. All samples, at the surface and at depth followed Redfield ratios closely with surface

waters having slightly higher DO and lower DIC concentrations than those at depth. Surface water DO concentrations were between 250 and ~280 μmoles kg^{-1}, while deeper waters ranged from ~230 to 255 μmoles kg^{-1}.

As stratification increased during the spring, production in the surface waters increased. As a result, DIC was drawn down and DO concentrations increased to a range between ~270 and 410 μmoles kg^{-1}. DO concentrations were amplified while DIC was reduced at stations in the northern-most regions of both arms. These samples deviated the most from the Redfield ratio, while the remaining samples adhered to the Redfield ratio. Below the surface layer, DO concentration throughout the bay ranged from ~250 to 280 μmoles kg^{-1}.

During the summer of 2012, the surface waters within the two arms and CB continued to diverge from Redfield. DIC concentrations within the more northern regions of the bay (EA, WA, and CB) were increasingly drawn down, while DO concentrations remained high, indicating strengthening productivity in the surface waters. Surface DO concentrations ranged from ~260 to ~410 μmoles kg^{-1}, while at depth DO was lower, varying from 200 - ~270 μmoles kg^{-1}.

3.4.5 Air–sea gas flux

While GLBA itself represents only a small portion of Alaska's coastal environment, the coastal ocean surrounding the GOA has been shown to act as an important sink for atmospheric CO_2 when averaged seasonally, with uptake of 2.5 to 4.0 mmoles C m^{-2} d^{-1} (Evans and Mathis, 2013). Monthly pCO_2 was averaged seasonally and regionally in GLBA to identify the spatial and temporal variability of air-sea CO_2 exchange between the atmosphere and the surface waters of the bay. Figure 3.7 shows the air-sea fluxes for the four regions of the bay during each season between the summers of 2011 and 2012, with positive fluxes indicating outgassing of CO_2 and negative fluxes representing uptake of CO_2 from the atmosphere into the surface waters.

During the summer of 2011, regions of oversaturation and undersaturation with respect to the atmospheric CO_2 were observed. Across the bay, winds were relatively low, at ~1.6 m s^{-1}, reducing turbulent wind mixing, allowing for stratification and, thus, primary production despite sustained tidal mixing within the bay. Surface waters of the CB and the WA were undersaturated with respect to atmospheric CO_2 with pCO_2 values of ~250 μatms. The CB has been observed to have abundant chl. *a* levels during most of the year (Hooge and Hooge, 2002), suggesting

enhanced primary production would act to decrease DIC concentrations and pCO_2 in this region. The WA also had diminished DIC concentrations during this summer largely due to the influx of low-macronutrient tidewater runoff. These lower DIC values caused the CB and the WA to act as minor sinks (~ -0.3 ± 0.02 mmoles C m^{-2} d^{-1} each). The LB and EA had much higher seawater pCO_2 values of ~488 µatms and ~463 µatms, respectively, causing these regions to act as a source for atmospheric CO_2 of ~0.2 ± 0.01 mmoles C m^{-2} d^{-1} for each region. In the lower and central regions of the bay surface water temperatures were relatively high at ~8.1°C and 8.5°C, respectively. Additionally, the LB experiences turbulent mixing due to tidal action across the shallow sill, which can act to inhibit strong stratification and enhance air-sea gas exchange. Within the EA it was likely the influence of low-TA glacial runoff that led to this region's source status. This runoff, low in TA, increased the pCO_2 in the surface waters. During this time of year seawater temperatures were also rising, increasing the pCO_2 of these waters. The combined influence of the reduced TA concentrations and increased temperatures resulted in an oversaturation of CO_2 in the seawater with respect to the atmosphere and overwhelmed any effect from DIC drawdown via primary production.

During the fall of 2011, winds increased slightly to ~2.0 m s^{-1} and surface waters in all regions of the bay were oversaturated with respect to the atmospheric CO_2. The LB experienced the highest pCO_2 at ~670 µatms and acted as the largest source for atmospheric CO_2 with a flux of ~1.10 ± 0.06 mmoles C m^{-2} d^{-1}. The CB also had elevated pCO_2 with ~510 µatms leading to outgassing of ~0.50 ± 0.03 mmoles C m^{-2} d^{-1}. The EA had a pCO_2 value similar to that of the CB (~514 µatms) as well as similar CO_2 flux of ~0.50 ± 0.03 mmoles C m^{-2} d^{-1}. Air-sea CO_2 flux in the WA was ~0.30 ± 0.02 mmoles C m^{-2} d^{-1}, similar to the EA and CB, but had a slightly lower pCO_2 of ~482 µatms. The high pCO_2 values observed during fall, despite strong DIC drawdown during summer, may have been the result of a variety of interactions. As a result of reduced glacial runoff during fall, TA concentrations increased (Reisdorph and Mathis, 2014). Additionally, surface water temperatures declined allowing them to hold more CO_2 while mixing brought DIC-rich waters from depth to the surface. These processes likely allowed more CO_2 retention in the water, thus increasing pCO_2 and making the bay a source for CO_2 to the atmosphere.

Similar to the fall, surface waters during the winter of 2012 were oversaturated in CO_2 with respect to the atmosphere and all regions experienced outgassing. pCO_2 values were more

constrained, especially within the arms and the CB, ranging from ~400 µatms in the WA and CB to ~432 µatms in the EA. Due to their similar pCO_2 values, as well as similar seawater temperatures (~3.5°C), the WA and CB experienced similar CO_2 fluxes of ~0.030 ± 0.002 and 0.060 ± 0.003 mmoles C m^{-2} d^{-1}. The EA had a slightly higher surface temperature (~4.1°C), which may have attributed to its higher flux of ~0.18 ± 0.01 mmoles C m^{-2} d^{-1}. The LB, which experienced the highest degree of turbulent mixing, especially seaward of the sill, had a CO_2 flux of ~0.76 ± 0.04 mmoles C m^{-2} d^{-1}. Despite winter having the lowest seawater temperatures, wind mixing peaked (~2.1 m s^{-1}) and allowed for CO_2-rich waters from depth to enter the surface waters, increasing pCO_2.

In the spring, seawater temperatures increased slightly to ~5°C across the bay while salinity remained similar to values observed during the winter (~29 to 31). However, during the spring, all regions, except for the LB, transitioned to sinks for atmospheric CO_2. pCO_2 in the LB remained oversaturated with respect to CO_2 at ~423 µatms and had a flux of ~0.11 ± 0.01 mmoles C m^{-2} d^{-1}, likely the result of greater turbulent flow seaward of the sill delaying the formation of strong stratification and inhibiting primary production. Within the other three regions of the bay, surface water temperatures increased slightly, by just over 1°C, but due to the onset of spring productivity DIC was drawn down in the surface waters, decreasing the pCO_2 and allowing them to become sinks for atmospheric CO_2. The EA had the greatest decrease in pCO_2, dropping from ~432 µatms to ~167 µatms and exhibiting seasonal outgassing of ~ -0.87 ± 0.04 mmoles C m^{-2} d^{-1} between the winter and spring. The WA and CB regions acted in a similar manner. The reduction in pCO_2 within these two regions was also the result of increased primary production drawing down DIC in the surface waters causing them to become a seasonal sink for CO_2, taking up ~ -0.39 ± 0.02 mmoles C m^{-2} d^{-1} in the CB and ~ -0.60 ± 0.03 mmoles C m^{-2} d^{-1} in the glacially-influenced WA.

During the summer of 2012, CO_2 over- and undersaturation of surface waters varied regionally, with surface waters in the northern regions becoming increasingly saturated with respect to atmospheric CO_2. While, pCO_2 in the EA did increase from the spring, it was still less than atmospheric at ~337 µatms causing ~ -0.13 ± 0.01 mmoles C m^{-2} d^{-1} of ingassing. The increase in pCO_2 may have been due to a small increase in seawater temperature of ~1°C coupled with a reduction in TA (Reisdorph and Mathis, 2014), overwhelming the drawdown in DIC from primary production. The CB was a stronger sink for CO_2 with a lower pCO_2 of ~200 µatms and a

flux of ~ -0.44 ± 0.02 mmoles C m^{-2} d^{-1}. This reduction in pCO_2 was likely due to high levels of primary production in CB, as it has been noted to have some of the highest chl. *a* levels, as well as high nutrient replenishment from tidal mixing between the mixed waters of LB and the stratified waters within the CB (Hooge and Hooge, 2002). The remaining regions, the LB and WA, acted as sources for atmospheric CO_2 during this summer with pCO_2 values of ~411 µatms and ~507 µatms, respectively. The LB experiences the highest degree of turbulent or tidal mixing across the sill, as well as seaward of the sill, inhibiting stratification and primary production and causing it act as a source for atmospheric CO_2 year-round. During the summer of 2012, the LB experienced a near-neutral flux of ~0.040 ± 0.01 mmoles C m^{-2} d^{-1}. The WA was also oversaturated with respect to atmospheric CO_2 with a pCO_2 of ~507 µatms and a flux of ~0.26 ± 0.01 mmoles C m^{-2} d^{-1}. The difference between the sink/source status of the east and west arms of the bay was likely the result of differences in glacial influences. The WA is much more influenced by low-TA glacial runoff as it has the majority of the tidewater glaciers along its length. During the summer of 2012, these glaciers caused a higher degree of TA dilution than was observed within the WA, a difference of ~100 µmoles kg^{-1}. The upper end of WA also had the lowest DIC concentrations observed during this summer also likely due to the high tidewater glacier runoff, which tends to be low in macronutrients.

3.5 Conclusions

GLBA experiences a high degree of spatial and temporal variability in biogeochemical characteristics throughout the year. Environmental influences vary seasonally along a gradient from the glacially-influenced northern regions within the arms to the marine-influenced LB. This imparts spatial differences in stratification and macronutrient availability that effect biological processes and thus, rates of NCP.

We have calculated regional NCP values for each seasonal transition from the summer of 2011 through summer 2012 for GLBA. Despite GLBA's limited exchange with the marine waters of the GOA, it has been observed to have elevated primary production through most of the year (Hooge and Hooge, 2002), perhaps due to tidal mixing. However, rapid deglaciation within GLBA over the past ~250 years has imparted a high volume of fresh glacial runoff, a portion of which has been from tidewater glaciers that melt directly into the bay, affecting stratification, macronutrient concentrations, and influencing air-sea CO_2 exchange.

Between the summers of 2011 and 2012, nutrient concentrations in GLBA tended to be lowest in the surface waters of the arms, though never reaching depletion, during the summer season when glacial runoff, primary production (Figure 3.2), and DO concentrations (Figure 3.6) were highest. Rates of NCP were highest during the transition between summer and fall of 2011, with regional NCP rates ranging from ~54 to ~80 mmoles C m^{-2} d^{-1}. Rates during the summer of 2012 were lower, between ~6 and ~20 mmoles C m^{-2} d^{-1}.

Between the fall of 2011 and winter of 2012, as well as between the winter and spring of 2012, air-sea gas exchange overwhelmed any production signal across the bay. The one exception was LB between winter and spring where NCP rates were positive, likely due to earlier replenishment of nutrients from marine source waters. Although air-sea flux overwhelmed NCP seasonally, fluxes were minimal, with maximum outgassing of ~1.1 mmoles C m^{-2} d^{-1} occurring in LB during the fall of 2011. While the direction of fluxes varied seasonally and regionally, LB acted as a small source for atmospheric CO_2 during all seasons of the study. During the summer of 2012, areas of CO_2 over- and undersaturation varied, with the LB and WA acting as sources for atmospheric CO_2 and the CB and EA acting as sinks. NCP followed this pattern with a maximum in the LB of 8.0×10^9 g C $season^{-1}$, followed by the CB with 8.5×10^8 g C $season^{-1}$. NCP was lowest within the WA (9.2×10^7 g C $season^{-1}$), likely due to low-TA, and low-macronutrient tidewater glacier runoff slowing primary production. Despite a sustained level of primary production in the WA, pCO_2 in this region remained oversaturated (~506 μatm) with respect to the atmosphere. This was attributed to the low-TA glacial runoff diluting TA concentrations in the surface water leading to elevated pCO_2. This, coupled with the fact that these warmer summer waters have inherently higher pCO_2, caused pCO_2 levels to remain elevated despite sustained biological production. It is clear from our observations that highly glaciated systems like GLBA behave much differently than open ocean regions, as well as glaciated systems with less restricted marine exchange like PWS, when it comes to CO_2 fluxes. The complex interactions between NCP, temperature and TA cause GLBA to behave much differently than the adjacent GOA, which has been shown to be a significant sink for atmospheric CO_2 (Evans and Mathis, 2013).

The impact of rapid deglaciation in GLBA can be observed in the seasonal impacts on the biogeochemistry of this marine system. The influence of surrounding glaciers, especially tidewater glaciers, has the potential to significantly impact the efficiency and makeup of the

marine food web within GLBA. Some prey species, such as capelin, thrive nearest the tidewater glaciers, most of which are currently receding and thinning, leaving these species with a smaller, less optimal habitat and affecting predators at higher tropic levels. A similar occurrence in the GOA saw a decline in predator species, such as harbor seals and red-legged kittiwakes, as the result of glacial recession (Arimitsu et al., 2008). The full impact that deglaciation has on a marine system like GLBA, and the numerous similar systems along the Alaskan GOA coast, is currently unknown. However, the coastal margin of the GOA has been estimated at ~3000 km, or ~1.5 times the length of the U.S. continental margin between northern Washington and southern California and, therefore, needs more study and should be considered an area of vital importance to the regional carbon budget.

3.6 Figures

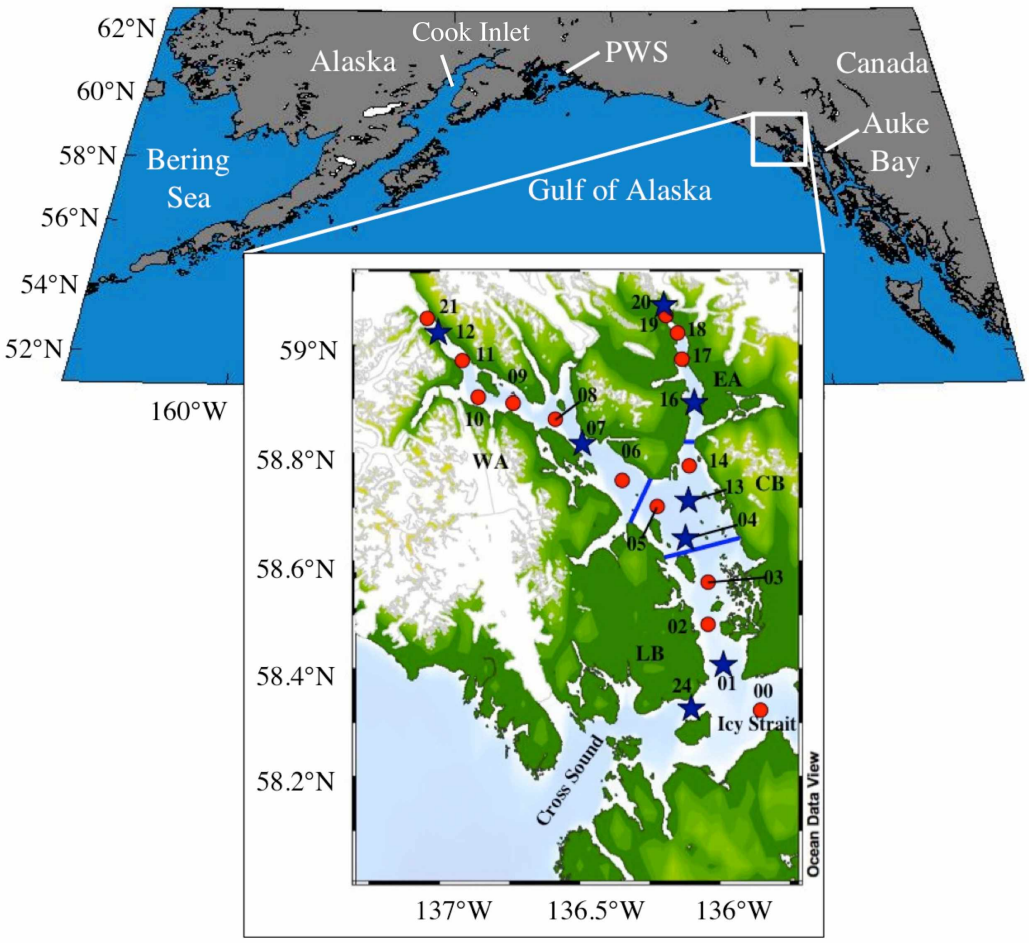

Figure 3.1 — Glacier Bay location and oceanographic sampling station map: Blue lines denote regional boundaries. Red dots show oceanographic station locations with station number. Blue stars represent 'core' station location. LB = lower bay, CB = central bay, EA = east arm, WA = west arm.

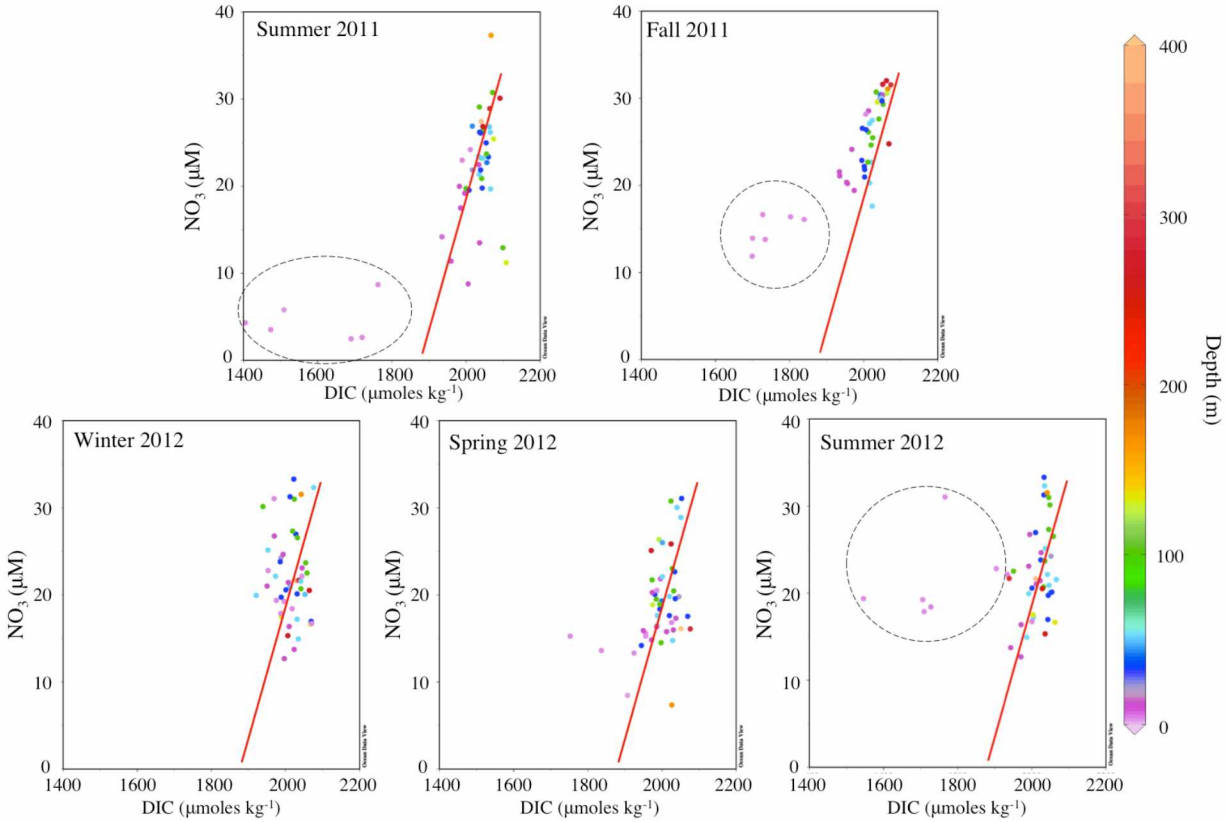

Figure 3.2 — Seasonal DIC vs. NO_3 vs. depth: Scatter plots of DIC concentrations vs. NO_3 concentrations for each season between the summer of 2011 and the summer of 2012. Color bar represents depth in m. The red line depicts the C:N Redfield ratio of 106:16. Dotted circles highlight samples that substantially deviate from Redfield.

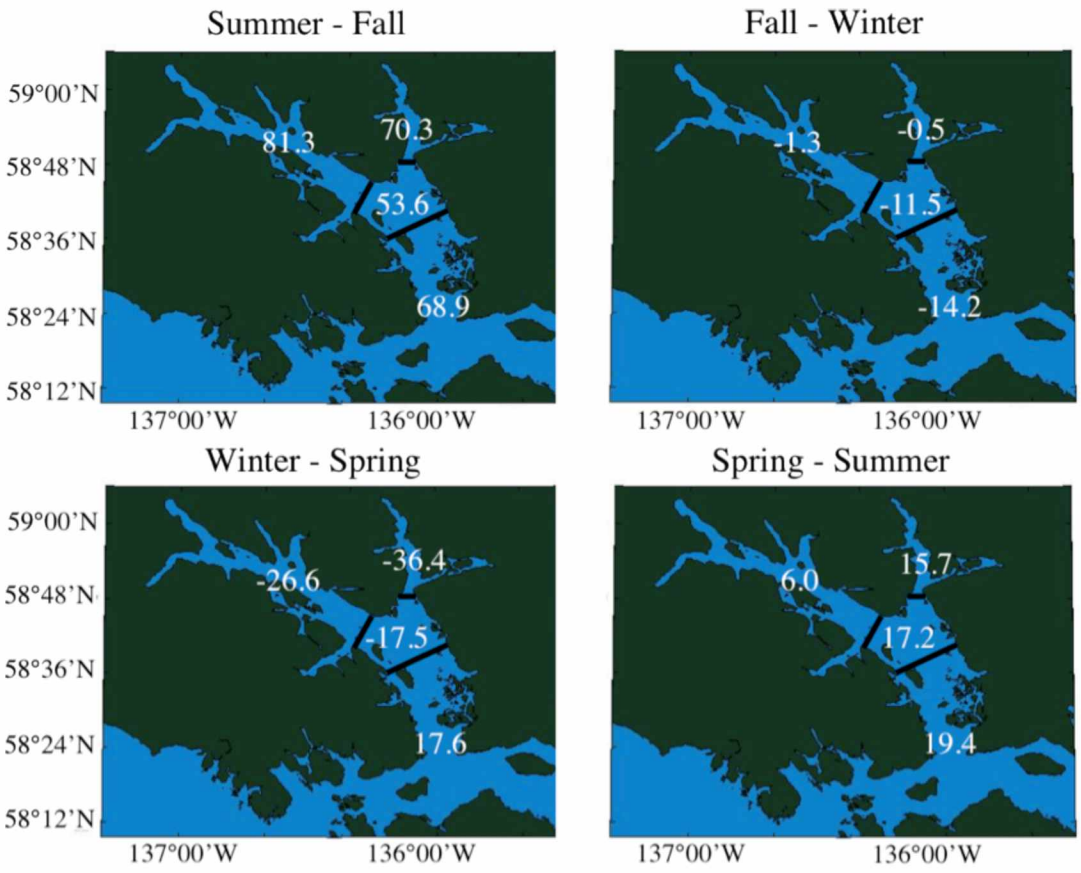

Figure 3.3 — Regional rates of net community production: Rates of NCP in mmoles C m^{-2} d^{-1} for seasonal transitions from summer to fall of 2011 in the upper left through the spring to summer of 2012 in the lower right.

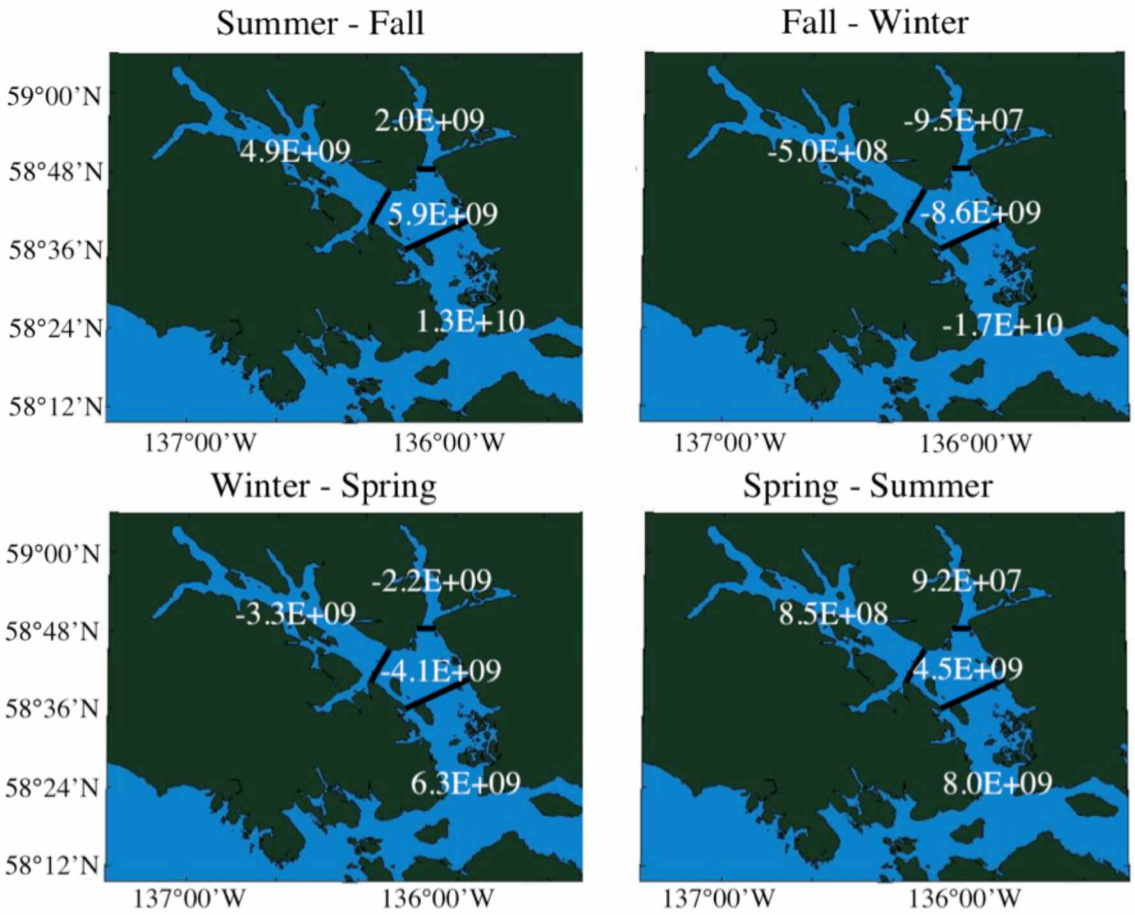

Figure 3.4 — Regional masses of net community production: Masses of NCP in g C season^{-1} for seasonal transitions from summer to fall of 2011 in the upper left through the spring to summer of 2012 in the lower right.

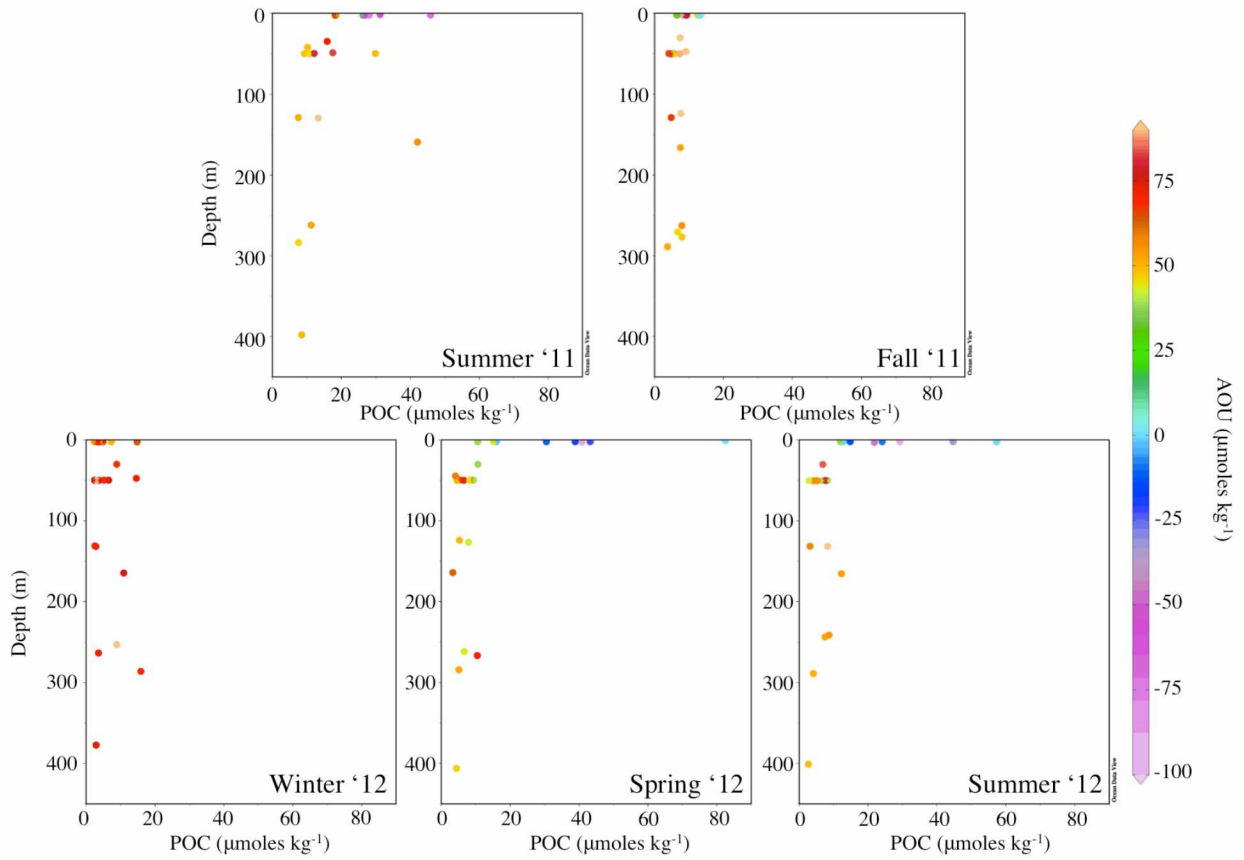

Figure 3.5 — Seasonal POC vs. depth vs. AOU: Seasonal scatter plots of POC concentrations vs. depth for each season between the summer of 2011 and the summer of 2012. Color bar represents AOU in µmoles kg^{-1}.

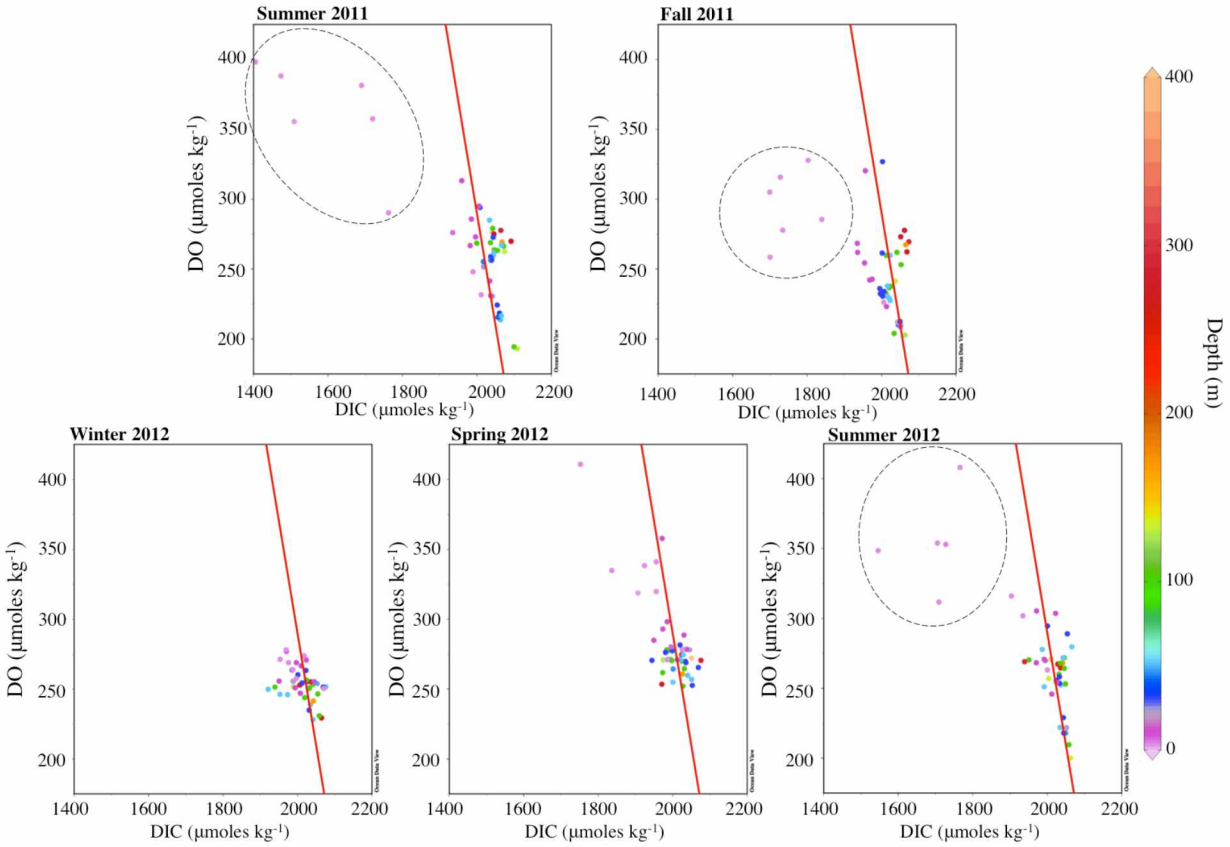

Figure 3.6 — Seasonal DIC vs. DO vs. depth: Scatter plots of DIC concentrations vs. DO concentrations for each season between the summer of 2011 and the summer of 2012. Color bar represents depth in m. The red line depicts the C:O Redfield ratio of 106: -170. Dotted circles highlight samples that substantially deviate from Redfield.

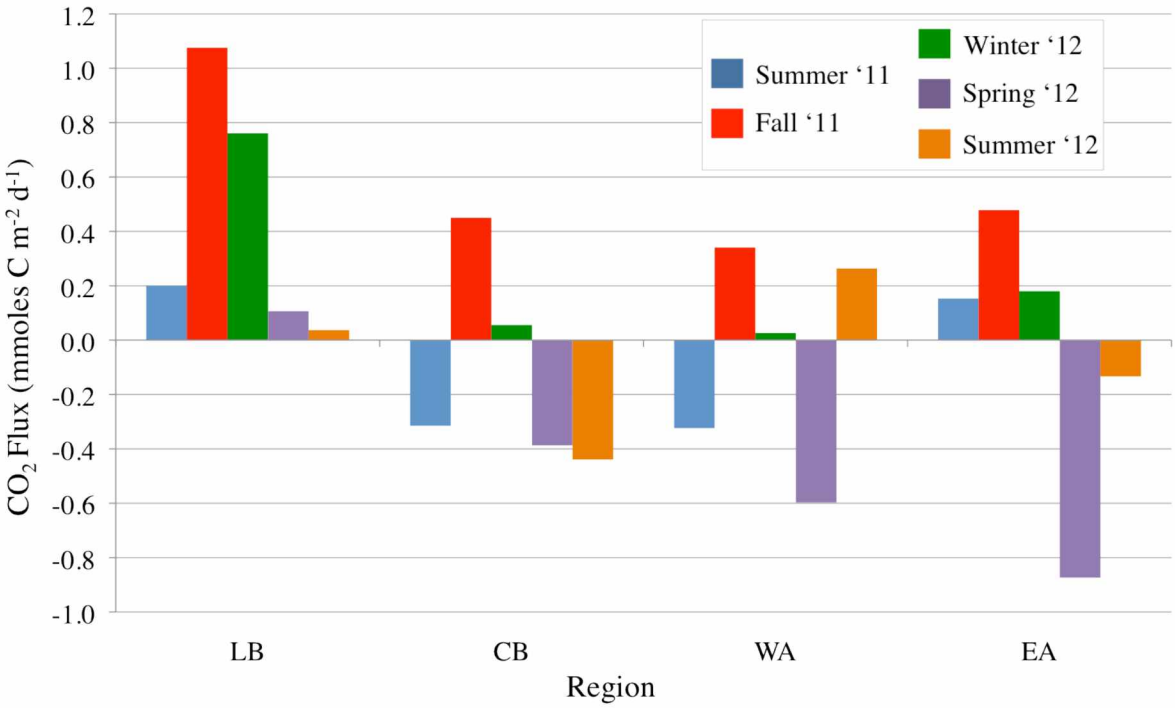

Figure 3.7 — Air-sea CO_2 flux: Seasonal air-sea CO_2 fluxes by region in mmoles C m^{-2} d^{-1}. Blue represents the summer of 2011, red = fall of 2011, green = winter of 2012, purple = spring of 2012, yellow = summer of 2012.

3.7 References

Anderson, L.A., Sarmiento, J.L., 1994. Redfield ratios of remineralization determined by nutrient data analysis. Global Biogeochem. Cycles, 8, 65–80.

Aracena, C., Lange, C.B., Luis Iriarte, J., Rebolledo, L., Pantoja, S., 2011. Latitudinal patterns of export production recorded in surface sediments of the Chilean Patagonian fjords (41–55°S) as a response to water column productivity. Cont. Shelf Res., 31, 340–355. doi:10.1016/j.csr.2010.08.008

Arimitsu, M.L., Piatt, J.F., Litzow, M.A., Abookire, A.A., Romano, M.D., Robards, M.D., 2008. Distribution and spawning dynamics of capelin (*Mallotus villosus*) in Glacier Bay, Alaska: a cold water refugium. Fish. Oceanogr., 17, 137–146. doi:10.1111/j.1365-2419.2008.00470

Bates, N.R., Best, M.H.P., Hansell, D.A., 2005. Spatio-temporal distribution of dissolved inorganic carbon and net community production in the Chukchi and Beaufort Seas. Deep Sea Res. Part II Top. Stud. Oceanogr., 52, 3303–3323. doi:10.1016/j.dsr2.2005.10.005

Cross, J.N., Mathis, J.T., Bates, N.R., 2012. Hydrographic controls on net community production and total organic carbon distributions in the eastern Bering Sea. Deep Sea Res. Part II Top. Stud. Oceanogr., 65–70, 98–109. doi:10.1016/j.dsr2.2012.02.003

Dickson, A.G., Millero, F.J., 1987. A comparison of the equilibrium constants for the dissociation of carbonic acid in seawater media. Deep Sea Res., 34, 1733–1743. doi:10.1016/0198-0149(87)90021-5

Dickson, A.G., 1990. Standard potential of the reaction: $AgCl_{(s)} + ½H_{2(g)} = Ag_{(s)} + HCl_{(aq)}$, and the standard acidity constant of the ion HSO_4^- in synthetic seawater from 273.15 to 318.15. Jour. of Chem. Thermodyn., 22, 113–127. doi:10.1016/0021- 9614(90)90074-Z

Engel, A., Goldthwait, S., Passow, U., Alldredge, A., 2002. Temporal decoupling of carbon and nitrogen dynamics in a mesocosm diatom bloom. Limnol. Oceanogr., 47, 753–761. doi:10.4319/lo.2002.47.3.0753

Etherington, L., Hooge, P.N., Hooge, E.R., Hill, D.F., 2007. Oceanography of Glacier Bay, Alaska: implications for biological patterns in a glacial fjord estuary. Estuar. & Coasts, 30, 927–944.

Evans, W., Mathis, J.T., 2013. The Gulf of Alaska coastal ocean as an atmospheric CO_2 sink. Cont. Shelf Res., 65, 52–63. doi:10.1016/j.csr.2013.06.013

Goering, J.J., Patton, C.J., Shiels, W.E., 1973. Primary production. In: Hood, D.W., Shiels, W.E., Kelley, E.J. (eds) Environmental studies of Port Valdez. Institute of Marine Science Occasional Publications No. 3, University of Alaska, Fairbanks, AK, 253–279.

Goñi, M.A., Teixeira, M.J., Perkey, D.W., 2003. Sources and distribution of organic matter in a river-dominated estuary (Winyah Bay, SC, USA). Estuar. Coast. Shelf Sci., 57, 1023–1048. doi:10.1016/S0272-7714(03)00008-8

Hill S.J. Ciavola, L. Etherington, M.J. Klaar, D.F., 2009. Estimation of freshwater runoff into Glacier Bay, Alaska and incorporation into a tidal circulation model. Estuar. Coast. Shelf Sci., 82, 95–107.

Hooge, E.R., Hooge, P.N., 2002. Fjord oceanographic processes in Glacier Bay, Alaska, Glacier Bay Report, Gustavus, AK, 1-144.

Kirchhoff, M.D., Lindell, J.R., Hodges, J.I., 2014. From critically endangered to least concern?—A revised population trend for the Kittlitz's Murrelet in Glacier Bay, Alaska. Condor, 116, 24–34. doi:10.1650/CONDOR-13-123.1

Lee, K., 2001. Global net community production estimated from the annual cycle of surface water total dissolved inorganic carbon. Limnol. Oceanogr., 46, 1287–1297. doi:10.4319/lo.2001.46.6.1287

Lewis, E., Wallace D.W.R., 1998. CO2SYS – program developed for CO_2 system calculations, Report ORNL/CDIAC-105 (Carbon Dioxide Information and Analysis Centre), Oak Ridge National Lab., U.S. Department of Energy.

Lockwood, D., Quay, P.D., Kavanaugh, M.T., Juranek, L.W., Feely, R.A., 2012. High-resolution estimates of net community production and air-sea CO_2 flux in the northeast Pacific. Global Biogeochem. Cycles, 26, 1–16. doi:10.1029/2012GB004380

Mathis, J.T., Bates, N.R., Hansell, D.A., Babila, T., 2009. Net community production in the northeastern Chukchi Sea. Deep Sea Res. Part II Top. Stud. Oceanogr., 56, 1213–1222. doi:10.1016/j.dsr2.2008.10.017

Mathis, J.T. and Questel, J.M., 2013. The impacts of primary production and respiration on the marine carbonate system in the Western Arctic: implications for CO_2 fluxes and ocean acidification. Cont. Shelf Res., 67, 42-51. doi: 10.1016/j.csr.2013.04.041

Mehrbach, C., Culberson, C.H., Hawley, J.E., Pytkowicz, R.M., 1973. Measurement of the apparent dissociation constants of carbonic acid in seawater at atmospheric pressure. Limnol. Oceanogr., 18, 897–907.

Musgrave, D.L., Halverson, M.J., Pegau, S.W., 2013. Seasonal surface circulation, temperature, and salinity in Prince William Sound, Alaska. Cont. Shelf Res., 53, 20–29. doi:10.1016/j.csr.2012.12.001

Piatt, J.F., Anderson, P., 1996. Response of common murres to the Exxon Valdez oil spill and long-term changes in the Gulf of Alaska marine ecosystem. Am. Fish. Soc. Symp., 18, 720–737.

Quigg, A, Nunnally, C., McInnes, A., Gay, S., Rowe, G., Dellapenna, T., Davis, R., 2013. Hydrographic and biological controls in two subarctic fjords: an environmental case study of how climate change could impact phytoplankton communities. Mar. Ecol. Prog. Ser., 480, 21–37. doi:10.3354/meps10225

Reisdorph, S.C., Mathis, J.T., 2014. The dynamic controls on carbonate mineral saturation states and ocean acidification in a glacially dominated estuary. Estuar. Coast. Shelf Sci., 144, 8–18.

Robards, M., Drew, G., Piatt, J., Anson, J.M., Abookire, A., Bodkin, J., Hooge, P., Speckman, S., 2003. Ecology of selected marine communities in Glacier Bay: zooplankton, forage fish, seabirds, and marine mammals. USGS Glacier Bay Report, Gustavus, AK, 1-156.

Schartau, M., Engel, A., Schroter, J., Thoms, S., Volker, C., Wolf-Gladrow, D., 2007. Modelling carbon overconsumption and the formation of extracellular particulate organic carbon. Biogeosci. Discuss., 4, 13–67.

Schlitzer, R., 2013. Ocean data view, http://odv.awi.de.

Syvitski, J.P.M., Burrell, D.C., Skei, J.M., 1987. Fjords: processes and products. Springer-Verlag Inc, New York.

Thomas, H., Schneider, B., 1999. The seasonal cycle of carbon dioxide in Baltic Sea surface waters. J. Mar. Syst., 22, 53–67.

Trites, A.W., Donnelly, C.P., 2003. The decline of Steller sea lions *Eumetopias jubatus* in Alaska. Mamm. Rev., 33, 3–28.

Uppström, L.R., 1974. The boron/chlorinity ratio of deep-sea water from the Pacific Ocean. Deep Sea Res., 21, 161–162. doi:10.1016/0011-7471(74)90074-6

Voss, M., Baker, A., Bange, H.W., Conley, D., Cornell, S., Deutsch, B., Engel, A., Ganeshram, R., Garnier, J., Heiskanen, A.S., Jickells, T., Lancelot, C., Mcquatters-Gollop, A., Middelburg, J., Schiedek, D., Slomp, C.P., Conley, D.P., 2011. Nitrogen processes in coastal and marine ecosystems, in: Sutton, M.A., Howard, C.M., Erisman, J.W., Billen, G., Bleeker, A., Grennfelt, P., van Grinsven, H., Grizzetti, B. (Eds.), The European Nitrogen Assessment. Cambridge University Press, New York, 147–176.

Wanninkhof, R., McGillis, W.R., 1999. A cubic relationship between air-sea CO_2 exchange and wind speed. Geophys. Res. Lett., 26, 1889–1892.

Weber, T.S., Deutsch, C., 2010. Ocean nutrient ratios governed by plankton biogeography. Nature, 467, 550–4. doi:10.1038/nature09403

Williams, P.J., 1993. On the definition of plankton production terms: edited by: Li, W.K.W. and Maestrini, S.Y., Measurements of primary production from the molecular to the global scale. ICES Mar. Sci. Symp., 197, 9-19.

Whitledge, T.E., Malloy, S.C., Patton, C.J., Wirick, C.D., 1981. Automated nutrient analyses in seawater. Upton, New York.

Whitney, F.A., 2011. Nutrient variability in the mixed layer of the subarctic Pacific Ocean, 1987–2010. J. Oceanogr., 67, 481–492. doi:10.1007/s10872-011-0051-2

Ziemann, D.A., Conquest, L.D., Olaizola, M., Bienfang, P.K., 1991. Interannual variability in the spring phytoplankton bloom in Auke Bay, Alaska. Mar. Biol., 109, 321-334.

Chapter 4: General Conclusions

Over the past two centuries, Glacier Bay, AK has experienced the rapid deglaciation of the Glacier Bay Ice Field, leaving numerous retreating alpine and tidewater glaciers in its wake. As these remaining glaciers continue to melt, the runoff will strongly affect the biogeochemistry of the marine ecosystem. The fresh glacier melt is low in TA, and upon entering the marine system, dilutes TA concentrations in the surface waters, making them more susceptible to decreasing pH. The melting tidewater glaciers enter the bay without interacting with terrestrial material that could add some amount of carbonate minerals and macronutrients into the runoff, leaving it with reduced concentrations of vital inorganic nutrients. The influence of this glacial runoff can be seen seasonally in the marine biogeochemistry of the bay, especially in the surface waters. While we observed the bay to be well-mixed during the winter of 2012, there was strong stratification during the spring and summer seasons as a result of increased solar radiation coupled with freshwater discharge. We found that the regions of the bay that experienced the highest input of glacial runoff directly corresponded to the areas of aragonite undersaturation or near-undersaturation, most notably the east and west arms where summer aragonite saturation states dropped below the saturation horizon (Ω). These areas also had the lowest rates of NCP.

Wind and tidal mixing also played a role in determining saturation states across the bay, especially during the fall and winter, as they force the low-TA waters south out of the arms and mixed DIC-rich waters from depth into the surface waters. This was most notable during the fall of 2011 when all surface waters of the bay were undersaturated with respect to aragonite. Though spatially and temporally variable, aragonite saturation states reached a minimum of 0.40 during the summer of 2011 in the surface waters of the upper east arm when glacial runoff was at a peak. Saturation state reached a maximum of 3.26 in the same region during the spring of 2012 as primary production increased, but before glacial melt reached its peak.

The influence of glacier runoff in GLBA has the potential to impact the food web. Since the surrounding glacial runoff is low in macronutrients, it can dilute concentrations in the surface waters and impact primary production and the efficiency of the marine food web. During our study, we estimated the highest rates of NCP between the summer and fall of 2011 (~54 to ~81 mmoles C m^{-2} d^{-1}). This correlated with elevated carbon production, especially within the lower bay where production was estimated at with ~1.3×10^{10} g C $season^{-1}$ with production bay-wide of ~2.6×10^{10} g C $season^{-1}$. During the seasonal transitions between fall and winter, as well as

between winter and spring, any production signal was overwhelmed by air–sea CO_2 flux, indicated by negative rates of NCP.

Areas of CO_2 outgassing varied spatially and temporally across GLBA. During our study, the lower bay was always a source for atmospheric CO_2, with peak outgassing of ~1.1 mmoles C m^{-2} d^{-1} during the fall of 2011. Moreover, during the fall the entire bay was a source for atmospheric CO_2. In spring, we observed the largest CO_2 sink of any season, especially in the east arm with uptake of ~0.87 mmoles C m^{-2} d^{-1}, while the central bay acted as a sink for a longer duration of time (spring 2012 and both summer seasons) than any other region.

As CO_2 concentrations in the atmosphere continue to rise, the uptake of CO_2 by the ocean will continue to reduce global ocean pH. However, our work has shown that in places like GLBA, CO_2 uptake is not the only driver of ocean acidification. Freshwater runoff, such as that from glaciers, is low in alkalinity and dilutes seawater's ability to buffer against changes in pH. In GLBA, as well as in numerous glacially-influenced fjord systems in Alaska and worldwide, these processes influence calcium carbonate Ω and have the potential to lead to unfavorable conditions for those organisms that use calcium carbonate for shell-building. The potentially harmful impact on these organisms, several of which are a vital part of the marine food web, can affect NCP and lead to restructuring of the ecosystems food web with unknown implications.